DNA methylation is indispensable for leukemia inhibitory factor dependent embryonic stem cells reprogramming

Baojiang Wu,[1,2,9,10] Yunxia Li,[1,2,9,10] Bojiang Li,[3,10] Baojing Zhang,[1,2,10] Yanqiu Wang,[1,2] Lin Li,[4,5] Junpeng Gao,[5] Yuting Fu,[1,2] Shudong Li,[6] Fuchou Tang,[5,7,8] Xihe Li,[1,2,9,]* and Siqin Bao[1,2,]*

[1]The State Key Laboratory of Reproductive Regulation and Breeding of Grassland Livestock, Inner Mongolia University, Hohhot, 010070, China

[2]Research Center for Animal Genetic Resources of Mongolia Plateau, College of Life Sciences, Inner Mongolia University, Hohhot, 010070, China

[3]College of Animal Science and Veterinary Medicine, Shenyang Agricultural University, Shenyang, 110866 China

[4]Guangdong Provincial Key Laboratory of Proteomics, Department of Pathophysiology, School of Basic Medical Sciences, Southern Medical University, Guangzhou 510515, China

[5]Beijing Advanced Innovation Center for Genomics and Biomedical Pioneering Innovation Center, College of Life Sciences, Peking University, Beijing 100871, China

[6]Cancer Research UK and Medical Research Council Oxford Institute for Radiation Oncology, Department of Oncology, University of Oxford, Oxford OX3 7DQ, UK

[7]Peking–Tsinghua Center for Life Sciences, Peking University, Beijing, 100871, China

[8]Ministry of Education Key Laboratory of Cell Proliferation and Differentiation, Beijing, 100871, China

[9]Inner Mongolia Saikexing Institute of Breeding and Reproductive Biotechnology in Domestic Animal, Huhhot, 011517, China

[10]These authors contributed equally

*Correspondence: lixh@life.imu.edu.cn; baosq@life.imu.edu.cn

Highlights and novelty

- **LIF alone supports ESCs self-renew and pluripotency in chemically defined media.**
- **L-ESCs re-establish the epigenetic memory in reprogramming.**
- **DNA methylation is indispensable for L-ESCs reprogramming.**
- **L-ESCs contribute to somatic tissues and germ cells in chimaeras.**

Abstract

Naïve pluripotency can be maintained by the 2i/LIF supplements (CHIR99021, PD0325901 and LIF), which primarily affect canonical WNT, FGF/ERK, and JAK/STAT3 signaling. However, whether one of these tripartite supplements alone is sufficient to maintain naïve self-renewal remain unclear. Here we show that LIF alone is sufficient to induce reprogramming of 2i/LIF cultured ESCs (2i/L-ESCs) to ESCs with hypermethylated state (L-ESCs). *In vitro*, upon withdrawal of 2i, 2i/L-ESCs overcome the epigenetic barrier and DNA hypermethylated, which accompanies transcriptional changes and subsequent establishment of epigenetic memory. Global transcriptome features also show that L-ESCs are close to 2i/L-ESCs and in a stable state between naïve and primed pluripotency. Notably, our results demonstrate that DNA methylation is indispensable for LIF-dependent mouse ESCs reprogramming and self-renew. LIF-dependent ESCs reprogramming efficiency is significantly increased in serum treatment and reduced in *Dnmt3a* or *Dnmt3l* knockout ESCs. Importantly, unlike epiblast and EpiSCs, L-ESCs contribute to somatic tissues and germ cells in chimaeras. Such simple culture system of ESCs is more conducive to clarify the molecular mechanism of ESCs *in vitro* culture.

Key Words

Embryonic stem cells; Leukemia inhibitory factor; Reprogramming; Epigenetic; Genomic imprinting; DNA methylation

Introduction

Mouse embryonic stem cells (ESCs) are isolated from the inner cell mass of the pre-implantation embryos (Evans & Kaufman, 1981; Martin, 1981). Since pluripotent mouse embryonic stem cells were first established four decades ago, various culture systems of ESCs have been developed including the initial feeder/serum/cytokines, then the feeder/serum/Leukemia inhibitory factor (LIF) or Bone morphogenetic protein 4 (BMP4) (Smith *et al*, 1988; Williams *et al*, 1988; Ying *et al*, 2003), and the recent 2i/LIF (two inhibitors CHIR99021, PD0325901 and LIF) (Ying *et al*, 2008). It is generally believed that the optimal culture condition for ground sate ESCs comprises three additive 2i/LIF supplements which affect canonical WNT, FGF/ERK, and JAK/STAT3 signals. It has been reported that combination of any two of these tripartite supplements was sufficient to maintain naïve self-renewal of ESCs (Hackett *et al*, 2017). However, whether any one of the tripartite supplements plays a critical role with unique critical targets and signaling for ESCs pluripotency and self-renew remain elusive.

LIF is the most pleiotropic member of the interleukin-6 family of cytokines, and utilizes a receptor that consists of the LIF receptor B and gp130 (Ohtsuka *et al*, 2015). LIF is able to activate three intracellular signaling pathway: the JAK/STAT pathway, the PI3K/AKT pathway, and the SH2 domain-containing tyrosine phosphatase/MAPK pathway. LIF can also have paradoxically opposite effects in different cell types including stimulating or inhibiting cell proliferation, differentiation and survival. Since LIF was detected in extract from the feeders and has been used for most mice ESCs medium, it has been fully demonstrated to be the important supplement for ESCs self-renewal and pluripotency (Gao *et al*, 2019; Smith, 2001; Williams *et al*, 1988; Yang *et al*, 2017a; Yang *et al*, 2017b; Ying *et al*, 2003; Ying *et al*, 2008). Nevertheless, essential LIF/STAT3 functions can be affected compensated by activation of canonical WNT signaling and inhibition of FGF/ERK in the established culture system for self-renewal of ESCs (Ohtsuka *et al*, 2015). However, the consequences LIF/STAT3 signaling alone and precise regulatory mechanisms for ESCs self-renew have remained largely elusive.

Mouse ESCs cultured in different culture conditions exhibit distinct DNA methylation patterns. The 2i/LIF cultured ESCs (2i/L-ESCs) are globally DNA hypomethylated, whereas ESCs are grown in classical medium containing feeders, serum and LIF (S/L-ESCs) show global DNA hypermethylation (Leitch *et al*, 2013; Stadler *et al*, 2011). Additionally, DNA methylation levels were shown to be reversible between S/L-ESCs and 2i/L-ESCs (Leitch *et al*, 2013). Recent research reported prolonged MEK1/2 suppression impairs the epigenetic and genomic integrity as well as the developmental potential of ESCs, in part through the downregulation of DNA methylation (Choi *et al*, 2017; Yagi *et al*, 2017). This suggests that DNA methylation plays an important role in ESCs and normal development. We also showed that hypermethylation is a key point for expended pluripotency of ESCs in chemical defined medium (Bao *et al*, 2018).

In this study, to identify which signaling pathway is indispensable during ESCs self-renewing process, we focus on the JAK/STAT3 signaling. We show that LIF alone is able to support mouse embryonic stem cells self-renew and pluripotency as well as developmental potency. Our data also suggest that DNA methylation was indispensable for LIF dependent mouse ESCs reprogramming and self-renew. The detailed analysis of LIF alone dependent mouse ESCs reprogramming provides mechanistic insight into global DNA (de)methylation and also provides a rich resource for future studies on ESCs *in vitro* culture.

Results

LIF alone supports ESCs self-renew and pluripotency in chemically defined media

Serum plus LIF (S/L) medium and 2i plus LIF (2i/LIF) medium (based N2B27) are two typical ESCs culture media. In particular, LIF was found in almost all mice ESCs culture media *in vitro*. Therefore, we sought to determine whether LIF alone is capable of driving continuous cycles of self-renew of ESCs in the absence of serum and 2i medium. In here, we used six Oct4-ΔPE-GFP (GOF/GFP, mixed background of MF1, 129/sv, and C57BL/6J strains) ×129/sv F1 mice (Yoshimizu *et al*, 1999) ESCs lines (W1, W2, W4, W5, W6 and SQ3.3), which were directly derived in 2i/L medium (passages 15-20) and then switched to

chemically defined LIF (1000 IU/ml) medium based on N2B27 (L-medium) (Figures 1A and S1A). Initially ESCs showed signs of differentiation, such as flattening of colonies and reduction of GOF/GFP positive (GOF/GFP$^+$) for pluripotency-related transcription factors *Oct4* (Figure 1B). However, in passages 3-5, some GOF/GFP$^+$ colonies similar to those in undifferentiated ESCs, began to survive during LIF dependent ESCs reprogramming (Figure 1B). Here we designated these LIF-dependent GOF/GFP$^+$ ESCs in chemically defined medium as L-ESCs. GOF/GFP$^+$ colonies increased gradually with further passages.

Next, we performed fluorescence-activated cell sorting (FACS) on multiple L-ESCs lines and the GOF/GFP$^+$ L-ESCs were replaced for further passaging. The percentage of several GOF/GFP$^+$ L-ESCs (passages, p14-p42) ranged from 56% to 99% (Figure S1B), the sex of the mouse ESCs were not determined. After two or more repeated FACS for each L-ESCs line, GOF/GFP$^+$ L-ESCs reached nearly 98% purity, which was similar to the control 2i/L-ESCs (Figure S1B). These data indicate that LIF alone can maintain FACS-purified GOF/GFP$^+$ L-ESCs in undifferentiated pluripotent state (Figures 1B and S1B) with stable growth over 40 passages (Figure S1C), and high alkaline phosphatase (AP) activity (Figure S1D). The established L-ESCs lines have normal karyotype (Figure 1C) and express pluripotent markers OCT4, SOX2, and NANOG confirmed by immunofluorescence (Figure 1D). As we all know, in mouse ESCs, < 1% of cells exhibit some features of 2-cell (2C) embryos, such as the expression of 2C specific transcripts (Li & Izpisua Belmonte, 2018; Macfarlan *et al*, 2012). Interestingly, L-ESCs also retained 2C features, such as ZSCAN4 and MERVL activities demonstrated by immunostaining (Figure S1E). It has been reported that both X chromosomes are active in female naive ESCs cells (Pasque *et al*, 2018; Schulz *et al*, 2014), interestingly our immunostaining showed no H3K27me3 foci in female L-ESCs, suggesting that both X chromosomes are activated (Figure S1F). These results suggest that L-ESCs possess most of the characteristics of 2i/L-ESCs.

For a further stringent test of the pluripotency of L-ESCs, we examined the ability of clone formation from single cell level. We observed that L-ESCs could form single cell derived colony in chemically defined LIF alone condition with high efficiency, comparable to those

from 2i/L-ESCs (Figure 1E). Furthermore, to examine how essential LIF is in maintaining L-ESCs, we withdraw LIF and then added JAK inhibitor I, and observed significantly impaired propagation of L-ESCs with rapid differentiation (Figure 1F). However, LIF withdrawal and JAK inhibitor addition did not affect the self-renew of 2i/L-ESCs until passages 10 (Figure 1G). Taken together, our results suggest that LIF is an important and essential regulator in the maintenance of L-ESCs. In contrast to the previous notion that LIF and 2i were both indispensable for ESCs self-renewal, and established unique ground state of ESCs, in this study we showed that LIF alone is capable to support ESCs for self-renew and proliferation over passage 40.

Global transcriptome features of L-ESCs

To examine whether L-ESCs have distinct molecular features, we carried out RNA sequencing (RNA-seq) on L-ESCs, 2i/L-ESCs, S/L-ESCs and EpiSCs. Unsupervised hierarchical clustering (UHC) and principal component analysis (PCA) show L-ESCs close to 2i/L-ESCs (Figures 2A and 2B) and appear to be at an intermediate state between naïve ESCs and primed EpiSCs (Figure 2A). Compared with L-ESCs and 2i/L-ESCs, L-ESCs differentially expressed genes were related to embryonic morphogenesis, cellular lipid metabolic process, pattern specification process, embryonic organ morphogenesis and DNA hypermethylation. Whereas 2i/L-ESCs differentially expressed genes were related to stem cell development, stem cell proliferation, wnt-protein binding, gamete generation and meiotic cell cycle phase (Figure 2C). This shows L-ESCs display distinct molecular features for pluripotency. Interestingly, Compared with L-ESCs, 2i/L-ESCs, S/L-ESCs and EpiSCs, among differentially expressed genes (Ernst & Bar-Joseph, 2006), 3,347 genes (profile 7) were significantly high expressed in L-ESCs and 2i/L-ESCs compared with S/L-ESCs and EpiSCs (Figure 2D). Notably, a total of 1,621 genes (profile 2) were significantly upregulated in 2i/L-ESCs, compared with L-ESCs, S/L-ESCs and EpiSCs (Figure 2D). These RNA-seq analyses suggest that L-ESCs are in a stable state between naïve and primed pluripotency.

L-ESCs exhibit DNA hypermethylation and reserve genomic imprints

ESCs cultured in 2i/LIF or in LIF plus serum supplemented media represent two states of pluripotency of ESCs. Despite their similarities in pluripotency, 2i/L and S/L-ESCs rely on different signaling pathways and display strong differences in transcriptional and epigenetic landscapes (Habibi *et al*, 2013; Joshi *et al*, 2015; Ter Huurne *et al*, 2017). Here, we asked whether there are different epigenetic marks among L-ESCs, 2i/L-ESCs and S/L-ESCs. Whole-genome bisulfite sequencing (WGBS) was performed and compared the DNA methylation profiling of L-ESCs with 2i/L-ESCs and S/L-ESCs. The levels of DNA methylation in L-ESCs (median CpG methylation of ~80%) were comparable to S/L-ESCs (median ~90%) and higher than 2i/L-ESCs (median ~30%) (Figure 3A). This DNA methylation occurs across most methylated regions including intragenic, intergenic, exon, intron, short and long interspersed nuclear elements (SINEs and LINEs, respectively) and long terminal repeats (LTRs) (Figure S2A). Additionally, expression of DNA methylation associated genes was assessed using qPCR. As expected, DNA methyltransferases *Dnmt3a* and *Dnmt3l* was significantly upregulated in GOF/GFP positive L-ESCs compared with GOF/GFP negative cells in L-ESCs reprogramming process (Figure S2B). Moreover, the transcriptional level of genes known to influence DNA methylation levels, such as *Prdm14* and *Nanog* were significantly downregulated in L-ESCs (Figure S2B).

Next, we examined the dynamic changes of DNMT3A level in the process of L-ESCs reprogramming. Interestingly, the protein level of DNMT3A was present in L-ESCs (Figures 3B and 3C). Upon withdrawal of PD and CH, heterogeneous expression of DNMT3A was detected in nuclei of L-ESCs reprogramming at day 5, and in long-term culture the DNMT3A protein level in L-ESCs was significantly increased (Figure 3B), consistent with the higher methylation in L-ESCs. These data is also consistent with the notion that PD promotes downregulation of DNA methylation (Choi *et al*, 2017; Yagi *et al*, 2017). Strikingly, DNMT3A was only present in GOF/GFP positive cells of L-ESCs but not in GOF/GFP negative cells, performed by western blot (Figure 3C). The results showed DNMT3A is important factor to regulate DNA methylation in L-ESCs which possess hypermethylation

state.

Proper genomic imprinting is essential for embryonic development (Plasschaert & Bartolomei, 2014; Wu *et al*, 2014). We further performed genomic imprinting analysis on L-ESCs, S/L-ESCs and 2i/L-ESCs. Notably, compared with 2i/L-ESCs, the DNA methylation levels at imprinting control regions (ICRs) were markedly higher in L-ESCs and were similar to S/L-ESCs (Figure 3D). Collectively, we conclude that L-ESCs exhibited global genomic hypermethylation and reserved genomic methylation in the majority of imprinting control regions.

Serum treatment increase the efficiency of LIF-dependent ESCs reprogramming

Since the S/L-ESCs possess high levels of DNA methylation (Habibi *et al*, 2013), we next asked if serum treatment (prior to reprogramming of L-ESCs) may enhance the DNA methylation and then increase the efficiency of LIF dependent L-ESCs reprogramming. Next, we switched 2i/L-ESCs to S/L-medium, after five days induction, then S/L-ESCs were cultured in LIF alone chemically defined medium (L-medium) to assess the LIF dependent L-ESCs reprogramming. Our result indicates that S/L induction for 5 days significantly increased the number of AP^+ colonies compared with 2i/L-ESCs (Figures 4A and S3A). Consistent with this, 1×10^5 cells were seeded into 24-well cell culture plate in L-medium, the number of GOF/GFP^+ colonies increased dramatically in S/L induction group compared with 2i/L-ESCs (Figure 4B). After 4 days culture in L-medium, flow cytometry analysis showed that the percentage of GOF/GFP^+ cells in S/L induction group was increased dramatically compared with 2i/L-ESCs (Figure 4C). Furthermore, we tested this reprogramming process of ASCs in LIF alone medium using our previously published hypermethylated ASCs (Bao *et al*, 2018; Wu *et al*, 2020) and show that ASCs can also be efficiently reprogrammed into LIF-dependent ESCs (Figures S3B and S3C).

DNA methylation is indispensable for L-ESCs self-renew

Next, we asked whether DNA methylation is critical for this reprogramming, and investigated roles of different DNA methyltransferase in the early reprogramming processes. We separated GOF/GFP$^+$ and GOF/GFP$^-$ L-ESCs from early reprogramming processes by FACS. As expected, *Dnmt3a* and *Dnmt3l* expression levels in GOF/GFP$^+$ L-ESCs were significantly higher than that in GOF/GFP$^-$ L-ESCs (Figure S2B), as well as the DNMT3A protein level (Figure 3C). Interestingly, we also found higher expression level of H3K36me3 in GOF/GFP$^+$ L-ESCs (Figure 4D). This result is consistent with H3K36me3 remarked by the guard of DNA methylation process (Xu *et al*, 2019).

To unequivocally demonstrate whether stable L-ESCs self-renewal depends on DNA methylation, we next examined the role of DNA methyltransferases (DNMTs) on the regulating L-ESCs self-renewal processes by DNMTs inhibitor 5-aza-2'-deoxycytidine (5-Aza). The 5-Aza has been widely used as a DNA methylation inhibitor to experimentally induce gene expression and cellular differentiation (Beyrouthy *et al*, 2009; Juttermann *et al*, 1994). We cultured 2i/L-ESCs and L-ESCs in their respective medium plus 5-Aza and observed morphological changes of both 2i/L-ESCs and L-ESCS. These 5-Aza treated 2i/L-ESCs retained typical dome-shaped clonal morphology and were able to stably propagate at least ten passages (Figures 5A and S4A). In addition, there were slightly changes on the expression level of pluripotent genes (including *Nanog*, *Sox2* and *Prdm14*) between 5-Aza treated 2i/L-ESCs and untreated 2i/L-ESCs (Figure S4B). However, 5-Aza treated L-ESCs were difficult to maintain its propagation and self-renewal when treated under the L-medium plus 5-Aza. There was a few GOF/GFP$^+$ L-ESCs survived after seven days upon 5-Aza treatment and cells underwent apoptosis eventually (Figure 5B). These data indicate that L-ESCs are sensitive to inhibition of DNA methyltransferase by 5-Aza.

To further investigate the important role of DNA methylation on LIF-dependent ESCs reprogramming processes, we used *Dnmt3a* knockout ASCs (*Dnmt3a*$^{-/-}$-ASCs) which were cultured in ABC/L medium (Bao *et al*, 2018) and *Dnmt3l* knockout ESCs (*Dnmt3l*$^{-/-}$-ESCs)

which were cultured in S/L medium and then switched to chemically defined LIF medium. As expected, all *Dnmt3a* and *Dnmt3l* knockout cells significantly reduced the efficiency of LIF-dependent ESCs reprogramming (Figures 5C and 5D). While wild type ESCs and ASCs derived L-ESCs show normal self-renew and proliferation, whereas the proliferation of *Dnmt3a*$^{-/-}$ and *Dnmt3l*$^{-/-}$ L-ESCs decreased dramatically (Figures 5C, 5D, S3A and S3C). Taken together, our data demonstrate that DNA hypermethylation promotes the induction of LIF-dependent ESCs reprogramming.

In vitro and *in vivo* differentiation ability of L-ESCs

An important criterion for pluripotent ESCs is the ability of *in vitro* and *in vivo* differentiation (De Los Angeles *et al*, 2015). Upon 2i and LIF withdrawal, pluripotent ESCs differentiate into three germ layers, mesoderm, endoderm, and ectoderm (Shen *et al*, 2008). We cultured 2i/L-ESCs and L-ESCs into N2B27 basic medium, without 2i/L and LIF. In these culture conditions, ESCs differentiate. After 3-day and 6-day differentiation, we performed quantitative qPCR analysis and immunostaining. Interestingly, after 3-day differentiation, the expression level of all mesoderm, endoderm, and ectoderm genes were significantly increased in L-ESCs compared with 2i/L-ESCs (Figure 6A). Compared with 3-day differentiation, 6-day treatment significantly increased mesoderm, endoderm, and ectoderm genes expression level in 2i/L-ESCs but not in L-ESCs (Figures S5A and S5B). This indicates that L-ESCs have strong flexibility and differentiation ability, expression of genes easy varied depends on the environment changes. Nevertheless, 6-day differentiation ability between 2i/L-ESCs and L-ESCs was not significant changes (Figure S5C). Meanwhile, we confirm protein levels of mesoderm, endoderm and ectoderm markers by immunostaining (Figure 6B). In addition, similar to 2i/L-ESCs, L-ESCs also generated teratomas that contained derivatives of the three germ layers (Figure 6C). The results showed that L-ESCs had the differentiation ability *in vitro* and *in vivo*.

Contribution of L-ESCs to full-term embryonic development

Finally, we tested the *in vivo* developmental potential of L-ESCs in chimeric embryos. Using

L-ESCs derived from 2i/L-ESCs, we injected L-ESCs into 8-cell stage embryos (Figure 7A). We noticed that L-ESCs were successfully integrated into E13.5 germlines of chimeras. Notably, 36.8% (7/19) of recovered embryos showed chimeric contribution and 57.1% (4/7) of chimeric embryos appeared germlines contribution (Figures 7B and 7C). We further tested whether it is possible to obtain L-ESCs-derived postnatal chimeric mice. Of all 20 born pups, 5 L-ESCs-derived chimeras (25%) were obtained (Figures 7D and 7E). Although the rate of chimeric contribution is lower in L-ESCs than 2i/L-ESCs, this was not seen with EpiSCs (Huang *et al*, 2012). Hence, these data demonstrate the pluripotency of L-ESCs and their chimeric competency to both germlines contribution and full-term development.

Discussion

Embryonic stem cells depend on extrinsic and intrinsic regulator, form the nature of pluripotency and also emerge spectrum of pluripotent states (Ying *et al*, 2003; Ying *et al*, 2008). The signaling of WNT, ERK and JAK/STAT3 are main regulator to combine to control pluripotency, however, precise function of individual signaling pathway is unclear (Ohtsuka *et al*, 2015). In this study, we represent the induction of one novel cell type, L-ESCs from 2i/L-ESCs, which depend on JAK/STAT3 signaling alone, and provide new insights on pluripotent stem cells. In particular, the L-ESCs show higher DNA methylation levels than 2i/L-ESCs (Figure 3A), and based on transcriptional level, L-ESCs appeared to be at an intermediate state between naïve ESCs and primed EpiSCs (Figure 2A). We also find that genomic imprints are more stable in L-ESCs relative to 2i/L-ESCs (Figure 3D). Based on the gene expression and DNA methylome analysis, L-ESCs appeared to be at an intermediate state between naïve ESCs and primed EpiSCs, and may represent the cells with the characteristics of the early postimplantation epiblast.

LIF signaling include JAK/STAT, MARK and PI(3)K pathway, and stimulates a states of differentiation, survival and self-renewal, and determines the fate of cells (Ohtsuka *et al*, 2015). In mouse ESCs, it is generally believed that LIF signaling is skewed towards survival and self-renewal, whereas activation of canonical WNT signaling and blockade of FGF/ERK

blocks cell differentiation (Ohtsuka *et al*, 2015). In this study we show that under LIF alone medium, some proportion of surviving ESCs acquire new features and describe these cells as L-ESCs. These cells maintained self-renewal and pluripotency over passage 40. We show that L-ESCs died in 10 days in medium with JAK inhibitor (Figures 1F and 1G). It has been clear that LIF is critical to L-ESCs self-renewal and to maintain undifferentiated state. It is interesting how LIF alone play such important roles in programming of L-ESCs. One hypothesize is that 2i/L-ESCs cultured in L-medium became heterogeneous, majority of 2i/L-ESCs differentiation in this regime, and only small proportion indicates the presence of naïve ESCs, which the JAK/STAT3 may favor to bind to cofactors or intrinsic factor that promote self-renew. Recently Ying et al reported STAT3 signaling functions in a binary "on/off" manner, however they used S/L medium, the defined mechanism needs to be further explored (Tai *et al*, 2014).

DNA methylation is of paramount importance for mammalian embryonic development and DNA methylation deficient embryos die at such an early stage of development (Greenberg & Bourc'his, 2019). Here, we show that DNA hypermethylation increase the efficiency of L-ESCs reprogramming in S/L medium, whereas *Dnmt3a* and *Dnmt3l* knockout model and 5-Aza treatment affect the efficiency of inducing L-ESCs reprogramming and self-renew. Interestingly, triple-knockout (TKO) mouse S/L-ESCs for *Dnmt1*, *Dnmt3a* and *Dnmt3b* exhibit DNA hypomethylation, grew robustly and maintained their undifferentiated characteristics (Tsumura *et al*, 2006). Unlike mouse ESCs, conventional 'primed' human ESCs cannot tolerate *Dnmt1* deletion, emphasizing the functional differences between mouse and human ESCs (Liao *et al*, 2015). We suggested that embryonic stem cells cultured in LIF alone exhibit media dependent DNA hypermethylation and this state support L-ESCs self-renew and proliferation. Notably, LIF-dependent ESCs reprogramming efficiency is significantly reduced in *Dnmt3a* or *Dnmt3l* knockout ESCs (Figure 7F). We also show that DNMT3A and H3K36me3 expression was higher in L-ESCs compare to 2i/L-ESCs. Recently multiple studies suggested that H3K36me3 participates in cross-talk with other chromatin marks, and promotes de novo DNA methylation by interacting with DNMTs and SETD2 (Xu *et al*, 2019). H3K36me3 are responsible for establishing and safeguarding the maternal

epigenome (Xu *et al*, 2019). Our result showed that H3K36me3 and DNMT3A were highly expressed in L-ESCs, the impact of H3K36me3 on the actual cellular functions at ESCs self-renewal or lineage differentiation, as well as the molecular mechanism, remains to be investigated in future.

Epigenetics including genomic imprinting has widespread roles in mammals, affecting embryonic and placental development and transmission of nutrients to the fetus, and regulating critical aspects of mammalian physiology, such as metabolism, neuronal development and adult behavior (Plasschaert & Bartolomei, 2014). We show here that L-ESCs reserve hypermethylated imprinting genes, and are easily differentiated in medium without LIF, which may suggest unique feature for ESCs pluripotency. On the other hand, unlike ASCs with high development potency in chimeras, a single L-ESCs do not contributes to development embryo, suggesting that L-ESCs state is intermediate between naïve ESCs and primed EpiSCs, and their pluripotency are more close to S/L-ESCs and EpiSCs. In conclusion, this study demonstrates LIF alone is capable to support mouse ESCs reprogramming and provides mechanistic insight into global DNA (de)methylation.

Acknowledgements

We are grateful to Dr Guoliang Xu for the gift of the *Dnmt3l* knockout ESCs. We thank Dr. Juan Li for critical reading of manuscript. This work was supported by grants from the Ministry of Science and Technology project of Inner Mongolia (20130216), the National Natural Science Foundation of China (No. 31560335), and the Ministry of Science and Technology of China (2017YFA0102702). Part of the bioinformatics analysis was performed on the Computing Platform of the Peking–Tsinghua Center for Life Science at Peking University. The authors declare that they have no conflict of interest.

Author contributions

B.W., F.T., X.L. and S.B. designed the experiments. B.W., Y.L., B.Z., Y.W. and Y.F. conducted the experiments; B.L. analysed the RNA-seq data. L.L. and J.G. prepared whole-genome

bisulfite sequencing experiment and analyses BS-seq data. S.L. helped proof to the manuscript. F.T., X.L., and S.B. who supervised different aspects of the paper.

Competing interests

The authors declare no competing interests.

References

Bao, S., Tang, W.W., Wu, B., Kim, S., Li, J., Li, L., Kobayashi, T., Lee, C., Chen, Y., Wei, M. *et al* (2018). Derivation of hypermethylated pluripotent embryonic stem cells with high potency. Cell Res *28*: 22-34.

Beyrouthy, M.J., Garner, K.M., Hever, M.P., Freemantle, S.J., Eastman, A., Dmitrovsky, E., and Spinella, M.J. (2009). High DNA methyltransferase 3B expression mediates 5-aza-deoxycytidine hypersensitivity in testicular germ cell tumors. Cancer Res *69*: 9360-9366.

Choi, J., Huebner, A.J., Clement, K., Walsh, R.M., Savol, A., Lin, K., Gu, H., Di Stefano, B., Brumbaugh, J., Kim, S.Y. *et al* (2017). Prolonged Mek1/2 suppression impairs the developmental potential of embryonic stem cells. Nature *548*: 219-223.

De Los Angeles, A., Ferrari, F., Xi, R., Fujiwara, Y., Benvenisty, N., Deng, H., Hochedlinger, K., Jaenisch, R., Lee, S., Leitch, H.G. *et al* (2015). Hallmarks of pluripotency. Nature *525*: 469-478.

Ernst, J., and Bar-Joseph, Z. (2006). STEM: a tool for the analysis of short time series gene expression data. BMC Bioinformatics *7*: 191.

Evans, M.J., and Kaufman, M.H. (1981). Establishment in culture of pluripotential cells from mouse embryos. Nature *292*: 154-156.

Gao, X., Nowak-Imialek, M., Chen, X., Chen, D., Herrmann, D., Ruan, D., Chen, A.C.H., Eckersley-Maslin, M.A., Ahmad, S., Lee, Y.L. *et al* (2019). Establishment of porcine and human expanded potential stem cells. Nat Cell Biol *21*: 687-699.

Greenberg, M.V.C., and Bourc'his, D. (2019). The diverse roles of DNA methylation in mammalian development and disease. Nat Rev Mol Cell Biol *20*: 590-607.

Habibi, E., Brinkman, A.B., Arand, J., Kroeze, L.I., Kerstens, H.H., Matarese, F., Lepikhov, K., Gut, M., Brun-Heath, I., Hubner, N.C. *et al* (2013). Whole-genome bisulfite sequencing of two distinct interconvertible DNA methylomes of mouse embryonic stem cells. Cell Stem Cell *13*: 360-369.

Hackett, J.A., Kobayashi, T., Dietmann, S., and Surani, M.A. (2017). Activation of Lineage Regulators and Transposable Elements across a Pluripotent Spectrum. Stem Cell Reports *8*: 1645-1658.

Huang, Y., Osorno, R., Tsakiridis, A., and Wilson, V. (2012). In Vivo differentiation potential of epiblast stem cells revealed by chimeric embryo formation. Cell Rep *2*: 1571-1578.

Joshi, O., Wang, S.Y., Kuznetsova, T., Atlasi, Y., Peng, T., Fabre, P.J., Habibi, E., Shaik, J., Saeed, S., Handoko, L. *et al* (2015). Dynamic Reorganization of Extremely Long-Range Promoter-Promoter Interactions between Two States of Pluripotency. Cell Stem Cell *17*: 748-757.

Juttermann, R., Li, E., and Jaenisch, R. (1994). Toxicity of 5-aza-2'-deoxycytidine to mammalian cells is mediated primarily by covalent trapping of DNA methyltransferase rather than DNA demethylation. Proc Natl Acad Sci U S A *91*: 11797-11801.

Leitch, H.G., McEwen, K.R., Turp, A., Encheva, V., Carroll, T., Grabole, N., Mansfield, W., Nashun, B., Knezovich, J.G., Smith, A. *et al* (2013). Naive pluripotency is associated with global DNA hypomethylation. Nat Struct Mol Biol *20*: 311-316.

Li, M., and Izpisua Belmonte, J.C. (2018). Deconstructing the pluripotency gene regulatory network. Nat Cell Biol *20*: 382-392.

Liao, J., Karnik, R., Gu, H., Ziller, M.J., Clement, K., Tsankov, A.M., Akopian, V., Gifford, C.A., Donaghey, J., Galonska, C. *et al* (2015). Targeted disruption of DNMT1, DNMT3A and DNMT3B in human embryonic stem cells. Nat Genet *47*: 469-478.

Macfarlan, T.S., Gifford, W.D., Driscoll, S., Lettieri, K., Rowe, H.M., Bonanomi, D., Firth, A., Singer, O., Trono, D., and Pfaff, S.L. (2012). Embryonic stem cell potency fluctuates with endogenous retrovirus activity. Nature *487*: 57-63.

Martin, G.R. (1981). Isolation of a pluripotent cell line from early mouse embryos cultured in medium conditioned by teratocarcinoma stem cells. Proc Natl Acad Sci U S A *78*: 7634-7638.

Ohtsuka, S., Nakai-Futatsugi, Y., and Niwa, H. (2015). LIF signal in mouse embryonic stem

cells. JAKSTAT *4*: e1086520.

Pasque, V., Karnik, R., Chronis, C., Petrella, P., Langerman, J., Bonora, G., Song, J., Vanheer, L., Sadhu Dimashkie, A., Meissner, A. *et al* (2018). X Chromosome Dosage Influences DNA Methylation Dynamics during Reprogramming to Mouse iPSCs. Stem Cell Reports *10*: 1537-1550.

Plasschaert, R.N., and Bartolomei, M.S. (2014). Genomic imprinting in development, growth, behavior and stem cells. Development *141*: 1805-1813.

Schulz, E.G., Meisig, J., Nakamura, T., Okamoto, I., Sieber, A., Picard, C., Borensztein, M., Saitou, M., Bluthgen, N., and Heard, E. (2014). The two active X chromosomes in female ESCs block exit from the pluripotent state by modulating the ESC signaling network. Cell Stem Cell *14*: 203-216.

Shen, X., Liu, Y., Hsu, Y.J., Fujiwara, Y., Kim, J., Mao, X., Yuan, G.C., and Orkin, S.H. (2008). EZH1 mediates methylation on histone H3 lysine 27 and complements EZH2 in maintaining stem cell identity and executing pluripotency. Mol Cell *32*: 491-502.

Smith, A.G. (2001). Embryo-derived stem cells: of mice and men. Annu Rev Cell Dev Biol *17*: 435-462.

Smith, A.G., Heath, J.K., Donaldson, D.D., Wong, G.G., Moreau, J., Stahl, M., and Rogers, D. (1988). Inhibition of pluripotential embryonic stem cell differentiation by purified polypeptides. Nature *336*: 688-690.

Stadler, M.B., Murr, R., Burger, L., Ivanek, R., Lienert, F., Scholer, A., van Nimwegen, E., Wirbelauer, C., Oakeley, E.J., Gaidatzis, D. *et al* (2011). DNA-binding factors shape the mouse methylome at distal regulatory regions. Nature *480*: 490-495.

Tai, C.I., Schulze, E.N., and Ying, Q.L. (2014). Stat3 signaling regulates embryonic stem cell fate in a dose-dependent manner. Biol Open *3*: 958-965.

Ter Huurne, M., Chappell, J., Dalton, S., and Stunnenberg, H.G. (2017). Distinct Cell-Cycle Control in Two Different States of Mouse Pluripotency. Cell Stem Cell *21*: 449-455 e444.

Tsumura, A., Hayakawa, T., Kumaki, Y., Takebayashi, S., Sakaue, M., Matsuoka, C., Shimotohno, K., Ishikawa, F., Li, E., Ueda, H.R. *et al* (2006). Maintenance of self-renewal ability of mouse embryonic stem cells in the absence of DNA methyltransferases Dnmt1, Dnmt3a and Dnmt3b. Genes Cells *11*: 805-814.

Williams, R.L., Hilton, D.J., Pease, S., Willson, T.A., Stewart, C.L., Gearing, D.P., Wagner, E.F., Metcalf, D., Nicola, N.A., and Gough, N.M. (1988). Myeloid leukaemia inhibitory factor maintains the developmental potential of embryonic stem cells. Nature *336*: 684-687.

Wu, B., Li, L., Li, B., Gao, J., Chen, Y., Wei, M., Yang, Z., Zhang, B., Li, S., Li, K. *et al* (2020). Activin A and BMP4 Signaling Expands Potency of Mouse Embryonic Stem Cells in Serum-Free Media. Stem Cell Reports *14*: 241-255.

Wu, T., Liu, Y., Wen, D., Tseng, Z., Tahmasian, M., Zhong, M., Rafii, S., Stadtfeld, M., Hochedlinger, K., and Xiao, A. (2014). Histone variant H2A.X deposition pattern serves as a functional epigenetic mark for distinguishing the developmental potentials of iPSCs. Cell Stem Cell *15*: 281-294.

Xu, Q., Xiang, Y., Wang, Q., Wang, L., Brind'Amour, J., Bogutz, A.B., Zhang, Y., Zhang, B., Yu, G., Xia, W. *et al* (2019). SETD2 regulates the maternal epigenome, genomic imprinting and embryonic development. Nat Genet *51*: 844-856.

Yagi, M., Kishigami, S., Tanaka, A., Semi, K., Mizutani, E., Wakayama, S., Wakayama, T., Yamamoto, T., and Yamada, Y. (2017). Derivation of ground-state female ES cells maintaining gamete-derived DNA methylation. Nature *548*: 224-227.

Yang, J., Ryan, D.J., Wang, W., Tsang, J.C., Lan, G., Masaki, H., Gao, X., Antunes, L., Yu, Y., Zhu, Z. *et al* (2017a). Establishment of mouse expanded potential stem cells. Nature *550*: 393-397.

Yang, Y., Liu, B., Xu, J., Wang, J., Wu, J., Shi, C., Xu, Y., Dong, J., Wang, C., Lai, W. *et al* (2017b). Derivation of Pluripotent Stem Cells with In Vivo Embryonic and Extraembryonic Potency. Cell *169*: 243-257 e225.

Ying, Q.L., Nichols, J., Chambers, I., and Smith, A. (2003). BMP induction of Id proteins suppresses differentiation and sustains embryonic stem cell self-renewal in collaboration with STAT3. Cell *115*: 281-292.

Ying, Q.L., Wray, J., Nichols, J., Batlle-Morera, L., Doble, B., Woodgett, J., Cohen, P., and Smith, A. (2008). The ground state of embryonic stem cell self-renewal. Nature *453*: 519-523.

Yoshimizu, T., Sugiyama, N., De Felice, M., Yeom, Y.I., Ohbo, K., Masuko, K., Obinata, M., Abe, K., Scholer, H.R., and Matsui, Y. (1999). Germline-specific expression of the Oct-4/green fluorescent protein (GFP) transgene in mice. Dev Growth Differ *41*: 675-684.

Figure Legends

Figure 1. LIF alone supports ESCs self-renew and pluripotency.

(A) Experimental outline of the L-ESCs derivation procedures from ESCs.

(B) 2i/L-ESCs were switched to L-medium and cultured to passages 3 (p3), p5, p25. Here we use 2i/L-ESCs with GOF/GFP reporter. Scale bars, 100 μm.

(C) Karyotyping of L-ESCs (p30).

(D) Immunostaining of OCT4, SOX2 and NANOG in L-ESCs. Scale bars, 50 μm.

(E) Single cell clonogenicity efficiency in L-ESCs.

(F) L-ESCs were treated with JAK inhibitor I after day 3 p2 and day 10 p4. Scale bars, 100 μm.

(G) 2i/L-ESCs were treated with JAK inhibitor I after day 3 p2, day 10 p6 and p10. Scale bars, 100 μm.

Figure 2. Analyses of molecular features of L-ESCs.

(A) Unsupervised hierarchical clustering (UHC) of the transcriptome from three biological replicates of four pluripotent stem cell lines.

(B) PCA analysis of gene expression of four pluripotent stem cells.

(C) Heatmap showing differentially expressed genes (mean log2(normalized read counts) > 2, log2(fold change) > 2, adjusted *p*-value < 0.05) in L-ESCs compared with 2i/L-ESCs. Significantly enriched GO terms and representative genes in each cluster are listed on the right.

(D) Compared with L-ESCs, 2i/L-ESCs, S/L-ESCs and EpiSCs, among differentially expressed genes, a total of 3,347 genes (profile 7) were significantly high expressed in L-ESCs and 2i/L-ESCs compared with S/L-ESCs and EpiSCs; a total of 1,621 genes (profile 2) were significantly upregulated in 2i/L-ESCs, compared with L-ESCs, S/L-ESCs and EpiSCs.

Figure 3. DNA methylation pattern of L-ESCs.

(A) DNA methylation level of 2 kilobase (kb) genomic tiles. Source data are provided in Table S1.

(B) Immunostaining of Dnmt3a in 2i/L-ESCs and different passages L-ESCs. Scale bars, 50 μm.

(C) Western blotting analysis for Dnmt3a in L-ESCs (GOF/GFP positive and negative cells).

(D) Heatmap showing DNA methylation level of ICRs in three different stem cells.

Figure 4. Serum improves the efficiency of L-ESCs reprogramming.

(A) Left: Alkaline phosphatase (AP) staining on 2i/L-ESCs and S/L-ESCs (2i/L-ESCs were cultured in S/L medium for 5 days) were switched to L-medium and after 10 days culture. Right: Quantification of number of AP positive colonies after 10 days culture. Error bars are mean ± SD (n = 5). *P* values were calculated by two tailed Student's *t*-test, $p < 0.05$.

(B) Left: GOF/GFP positive colonies on 2i/L-ESCs and S/L-ESCs (2i/L-ESCs were cultured in S/L medium for 5 days) were switched to L-medium and after 8 days culture. Scale bars, 100 μm. Right: Quantification of number of GOF/GFP positive colonies after 8 days culture. Error bars are mean ± SD (n = 4). *P* values were calculated by two tailed Student's *t*-test, $p < 0.05$.

(C) Left: Fluorescence-activated cell sorting (FACS) based on GOF/GFP positive cells, after 2i/L-ESCs and S/L-ESCs (2i/L-ESCs were cultured in S/L medium for 5 days) were switched to L-medium and after 4 days culture. Right: Quantification of Percentage of GOF/GFP positive cells after 4 days culture. Error bars are mean ± SD (n = 3). *P* values were calculated by two tailed Student's *t*-test, $p < 0.05$.

(D) Western blotting analysis for H3K36me3 in L-ESCs (GOF/GFP positive and negative cells).

Figure 5. DNA methylation is indispensable for L-ESCs self-renew.

(A) 2i/L-ESCs were treated with 5-Aza after 3 and 7 days, 2i/L-ESCs retained typical dome-shaped clonal morphology. Scale bars, 100 μm.

(B) L-ESCs were treated with 5-Aza after 3 and 7 days, there was a few GOF/GFP^{+} L-ESCs survived after 7 days 5-Aza treatment and to apoptosis in final. Scale bars, 100 μm.

(C) Left: GOP/GFP positive colonies on wild type ASCs and *Dnmt3a*$^{-/-}$ ASCs were switched to L-medium and after 10 days culture. Right: Quantification of number of GOP/GFP positive

colonies after 10 days culture. Error bars are mean ± SD (n = 8). *P* values were calculated by two tailed Student's *t*-test, $p < 0.05$.

(D) Left: AP staining on wild type ESCs and *Dnmt3l*$^{-/-}$ ESCs were switched to L-medium and after 8 days culture. Right: Quantification of number of AP positive colonies after 8 days culture. Error bars are mean ± SD (n = 8). *P* values were calculated by two tailed Student's *t*-test, $p < 0.05$.

Figure 6. The pluripotency of L-ESCs *in vivo* and *in vitro*.

(A) Relative expression of mesoderm, endoderm and ectoderm genes measured by qPCR, after L-ESCs were 3 days *in vitro* differentiation. Error bars are mean ± SD (n = 3). *P* values were calculated by two tailed Student's *t*-test, $p < 0.05$.

(B) Immunostaining of T, SOX17 and NESTIN, after 2i/L-ESCs and L-ESCs were 3 days *in vitro* differentiation. Scale bars, 50 μm.

(C) Mature teratomas from L-ESCs. Left: mesoderm, muscle like cells; middle: endoderm, gland like cells; right: ectoderm, epidermis like cells. The sections were stained with haematoxylineosin. Scale bars, 50μm.

Figure 7. Ability of L-ESCs to full-term embryonic development.

(A) Schematic of eight cell embryos injection protocol.

(B) Germline transmission of L-ESCs in E13.5 chimeras. PGCs were shown by GOF/GFP-positive cells (arrow). black arrow: mesonephros; white arrow: gonad; yellow arrow: gonadal PGCs. Scale bars, 100 μm.

(C) Summary of E13.5 chimera assays by L-ESCs injection. The black bar chart shows the percentages of chimeras among the collected E13.5 conceptuses, embryonic tissues (Em); gray bar, integration into primordial germ cells (PGCs) among the recovered E13.5 chimeras.

(D) Chimeric pups generated by injecting L-ESCs in ICR host blastocysts.

(E) The summary of full term chimeric pups were derived by L-ESCs.

(F) Schematic of DNA methylation affects LIF dependent embryonic stem cells reprogramming process.

Supplementary figures

Figure S1. Characteristics of L-ESCs

(A) Derivation of L-ESCs from 2i/L-ESCs.

(B) The summary of fluorescence-activated cell sorting (FACS) based on GOF/GFP positive cells in different passages L-ESCs.

(C) Morphology of L-ESCs at p43.

(D) Alkaline phosphatase (AP) staining on L-ESCs (p24). Scale bars, 100 μm.

(E) Immunostaining of MERVL and ZSCAN4 in 2i/L-ESCs and L-ESCs. Scale bars, 50 μm.

(F) Immunostaining of H3K27me3 in2i/L-ESCs and L-ESCs. Scale bars, 50 μm.

Figure S2. Upregulation of DNA methylation level in L-ESCs

(A) DNA methylation level at various genomic features.

(B) Relative expression of *Dnmt3a* and *Dnmt3l* measured by qPCR in GOF/GFP positive and negative L-ESCs; Relative expression of *Prdm14* and *Nanog* measured by qPCR in 2i/L-ESCs, S/L-ESCs and L-ESCs. Error bars are mean ± SD (n = 3). *P* values were calculated by two tailed Student's *t*-test, $p < 0.05$.

Figure S3. Serum improves the efficiency of L-ESCs reprogramming

(A) Derivation of L-ESCs from 2i/L-ESCs after 5 days S/L medium culture.

(B) Summary of AP positive cloning numbers on 2i/L-ESCs, ASCs and L-ESCs, when 2,000 cells were seeded into 6-well cell culture plate and 6 days culture.

(C) ASCs can be efficiently reprogrammed into LIF-dependent ESCs.

Figure S4. DNA methylation is indispensable for L-ESCs self-renew

(A) 2i/L-ESCs were treated with 5-Aza after p10, 2i/L-ESCs retained typical dome-shaped clonal morphology. Scale bars, 100 μm.

(B) Relative expression of *Nanog*, *Sox2* and *Prdm14* measured by qPCR in 2i/L-ESCs after 3 days 5-Aza treatment. Error bars are mean ± SD (n = 3). *P* values were calculated by two tailed Student's *t*-test, $p < 0.05$.

Figure S5. The pluripotency of L-ESCs *in vivo* and *in vitro.*

(A) Relative expression of mesoderm, endoderm and ectoderm genes measured by qPCR, after 2i/L-ESCs were 3 days and 6 days *in vitro* differentiation. Error bars are mean ± SD (n = 3). *P* values were calculated by two tailed Student's *t*-test, $p < 0.05$.

(B) Relative expression of mesoderm, endoderm and ectoderm genes measured by qPCR, after L-ESCs were 3 days and 6 days *in vitro* differentiation. Error bars are mean ± SD (n = 3). *P* values were calculated by two tailed Student's *t*-test, $p < 0.05$.

(C) Relative expression of mesoderm, endoderm and ectoderm genes measured by qPCR, after 2i/L-ESCs and L-ESCs were 6 days *in vitro* differentiation. Error bars are mean ± SD (n = 3). *P* values were calculated by two tailed Student's t-test, $p < 0.05$.

Material and methods

Mice

Oct4-ΔPE-GFP (GOF/GFP) transgenic mice (Yoshimizu et al., 1999) were used here with a mixed background of MF1, 129/sv, and C57BL/6J strains. All the animal experiments were performed following the ethical guidelines approved by Animal Research Committee of Inner Mongolia University, China.

Derivation of 2i/L-ESCs

Mouse embryos blastocysts (E3.5) were isolated from 129/sv females mated with GOF/GFP transgenic males. Green fluorescence indicated that GFP expression of the reporter is under the control of *Oct4* promoter and distal enhancer. This GFP transgene shows expression in the ICM of blastocysts and PGC *in vivo*, and in ESCs (Yoshimizu et al., 1999). ESCs culture medium consists of N2B27 medium (Life technology) supplemented with PD0325901 (PD, 1 μM, Miltenyi Biotec), CHIR99021 (CH, 3 μM, Miltenyi Biotec) and leukemia inhibitory factor (LIF, 1000 IU/ml, Millipore), henceforth were called 2i/L medium. Zona pellucida of blastocysts were removed by Acidic Tyrode's Solution (Sigma-Aldrich), and then placed to 24-well fibronectin-coated (FN, 16.7 μg/ml, Millipore) plate with 2i/L medium. ICM of blastocysts cultures grew efficiently and formed outgrowing colonies in 5-7 days culture. The resulting colonies were further cutting into smaller pieces by glass needles after 5-7 days culture, and then the colonies passaged by Accutase (Life technology) regularly on at every 2 days interval.

Derivation of L-ESCs

1×10^5 2i/L-ESCs were switched on fibronectin-coated (16.7 μg/ml, Millipore) 24-well cell culture plate containing L-medium which are N2B27 medium supplemented with leukemia inhibitory factor (1000 IU/ml, Millipore), and we call these cells as L-ESCs. Dependent on cell growth, L-ESCs were passage every other day in the early stage. After being cultured for 4-5 passages or 14-42 passages, GOF/GFP positive and negative L-ESCs were purified by flow-cytometry sorting by BD FACSAria (BD Biosciences) and further analysis. GOF/GFP positive purified L-ESCs were passage every other day treated with Accutase (Life

technology). L-ESCs were capable of self-renewal for over 40 passages. For inhibitor treatment experiment, we added JAK inhibitor I (0.6 μM, Calbiochem) or 5-Aza (6 μM, Sigma) into L-ESCs culture medium.

Derivation of S/L-ESCs

2i/L-ESCs were switch to fibronectin-coated plate with standard ES medium (Knockout DMEM; Knockout Dulbecco's modified Eagle's medium) supplemented with 20% fetal calf serum, 0.1 mM 2-mercaptoethanol, 2 mM L-glutamine, 0.1 mM non-essential amino acid, 50 U/ml Penicillin/Streptomycin and 1000U/ml LIF without feeder cells, we named these cells as S/L-ESCs.

Cell differentiation

2i/L-ESCs and L-ESCs were cultured in N2B27 medium for 3 to 6 days withdrawal of PD, CH and LIF, and LIF respectively.

Colony formation assay

Single 2i/L-ESCs and L-ESCs were seeded at a fibronectin-coated 96-well plates using mouth pipette, containing 2i/L and L-medium, respectively. The cells were cultured for 10 days and the number of colonies was assessed.

Western blot

Cells were collected with Accutase (Life technology), washed three times with DPBS, and lysed in buffer that contained 20 mM Tris (pH 8.0), 137 mM NaCl, 100 g/l glycerol, 50 g/l Triton X-100, and 4 g/l EDTA; 1 μl PMSF (0.1 M) and 10 μl phosphatase inhibitor (10 g/l) were added per 1 ml lysis buffer immediately before use. Proteins were denatured with 2 × SDS at 95 °C for 5 min. A total of 20 μg denatured protein was run on 8% or 10% SDS–PAGE gel and transferred to polyvinylidene difluoride (PVDF) membrane. Membranes were blocked with 5% nonfat milk in 1 ×TBS with 0.05% Tween-20 (TBST) for 1h. Samples were probed with primary antibodies overnight at 4℃. The primary antibodies used were anti-DNMT3A (CST, 3598S; dilution 1:1,000), anti-H3K36me3 (Abcam, ab9050; working

concentration, 1 μg/ml), and anti-β-ACTIN (Abcam, ab8227; dilution 1:5,000). Blots were rinsed with TBST. Membranes were incubated with HRP-conjugated secondary antibodies for 60 min at room temperature, and proteins were detected by ECL plus reagent. After rinsing with TBST, Clarity™ Western ECL Substrate (BIO-RAD) was used for visualization, and ChemiDoc™ MP Imaging System (BIO-RAD) was used for band detection.

Alkaline phosphatase (AP) staining

AP staining was carried out using AP staining kit from Sigma (86R-1KT) according to manufacturer's instructions. Briefly, the cells were fixed by 4% paraformaldehyde for 10 min, and then were stained by AP staining solution for overnight at room temperature.

Immunostaining

Cultured ESCs were briefly washed with PBS and fixed in 4% paraformaldehyde in PBS for 15 min at room temperature. Cells were permeabilized for 30 min with 1% BSA and 0.1% Triton X-100 in PBS. Antibody staining was carried out in the same buffer at 4℃ for overnight. The slides were subsequently washed three times in 1% BSA, 0.1% Triton X-100 in PBS (5 min each wash), were incubated with secondary antibody for 1h at room temperature in the dark, washed once for 5 min in 1% BSA, 0.1% Triton X-100 in PBS and twice for 5 min in PBS. The slides were then mounted in Vectashield with DAPI (Vector Laboratories) and imaged using a Olympus FV1000 confocal microscope. Primary antibodies used were: anti-OCT4 (BD Biosciences, Catalog Number: 611203, 1:200), anti-NANOG (eBioscience, Catalog Number: 14-5761, 1:500), anti-SOX2 (Santa cruz, Catalog Number: sc-17320, 1:200), anti-H3K27me3 (Upstate, Catalog Number: 07-449, 1:500), anti-ZSCAN4 (Abcam, Catalog Number: ab106646, 1:200), anti-MERVL (HuaAn Bio, Catalog Number: ER50102, 1:100), anti-DNMT3A (abcam, Catalog Number: ab79822, 1:500), anti-NESTIN (BOSTER Bio, Catalog Number: BM4494, 1:50), anti-BRACHYURY (R＆D Systems, Catalog Number: AF2085, 1:100) and anti-SOX17 (R＆D Systems, Catalog Number: AF1924, 1:100). All secondary antibodies used were Alexa Fluor highly crossed adsorbed (Molecular Probes).

Flow cytometry

GOF/GFP ESCs were harvested by Accutaes and sorting by BD LSRFortessa. Green fluorescence indicated that GFP expression of the reporter is under the control of Oct4 promoter and distal enhancer. This GFP transgene shows expression in the ICM of blastocysts and PGCs in vivo, and in ESCs. No GOF/GFP ESCs were used for FACS gating negative control. Measure fluorescence (detector 488 nm channel for GFP) by flow cytometer. Gating out of residual cell debris and measure diploid and tetraploid DNA peaks. A region representing GFP-positive cells were used to identifiy living cells and collected.

Teratomas formation

The 2i/L-ESCs and L-ESCs were disaggregated using Accutase, and 1×10^6 cells were injected into under epithelium of NOD–SCID mice. Three to five weeks after transplantation, tumor(s) were collected and fixed with 4% paraformaldehyde, and processed for paraffin sectioning. Sections were observed following Hematoxylinand Eosin staining.

Karyotyping

ESCs were prepared for cytogenetic analysis by treatment with colcemid (Sigma) at a final concentration of 0.1 μg/ml for 3h to accumulate cells in metaphase. Cells were then exposed to 0.075 M KCl for 25 min at 37℃ and fixed with 3:1 methanol: acetic acid. Air-dried slides were generated and G-banded following standard GTG banding protocols.

Production of chimeras

8-10 ESCs were injected gently into the ICR mice eight-cell stage embryos using a piezo-assisted micromanipulator attached to an inverted microscope. The injected embryos were cultured in KSOM medium (Millipore) at 37℃ in a 5% CO_2 atmosphere for overnight and then transferred to the uteri of pseudopregnant ICR mice at 2.5 days post coitus (dpc). The embryos were isolated at embryonic stage E13.5 and check germline transmission. Full term chimeras were confirmed by the coat color pattern of the pups at birth.

Real-time PCR

Total RNA was isolated with the RNeasy Plus Mini Kit (Qiagen) and reverse transcribed into cDNA using the Reverse Transcription System (Promega) according to the manufacturer's instructions. Quantitative real-time PCR (qRT-PCR) was conducted using a LightCycler® 96 Instrument (Roche Molecular Systems) and qRT-PCR reaction was performed with KAPA SYBR FAST qPCR kit (KAPA Biosystems). At least triplicate samples were assessed for each gene of interest, and GAPDH was used as a control gene. Relative expression levels were determined by the $2^{-\Delta\Delta Ct}$ method. Primer sequences used are given in Table S2.

Generation of *Dnmt3a* knockout ASCs lines

Guide RNA sequences were cloned into the plasmid px459 (Addgene, 62988). px459 containing *Dnmt3a* gRNAs were co-transfected into digested single ASC by Lipofectamine 2000 (Thermo Fisher Scientific). Single cell derived colonies were picked and expanded individually. Genomic DNA of colonies were extracted using the DNeasy Blood & Tissue Kit, which was further analyzed by genomic PCR. Colonies with the deletion of *Dnmt3a* locus were identified. *Dnmt3a* knockout ASCs (*Dnmt3a*$^{-/-}$ ASCs) were cultured in ABCL medium without puromycin. Guide RNA sequences and genotyping primer sequences used are given in Table S2.

RNA extraction and sequencing

Total RNA were extracted from approximately one million to two million cells using RNeasy Mini Kit (QIAGEN) according to the recommendation of manufacturer and then NEBNext® Poly (A) mRNA Magnetic Isolation Module was used to isolate mRNA from total RNA. Using mRNA as input, the first and second strand cDNAs were synthesized by NEBNext® RNA First Strand Synthesis Module and NEBNext® Ultra II Non-Directional RNA Second Strand Synthesis Module, respectively. Final libraries were prepared using KAPA Hyper Prep Kits (8 PCR cycles) and sequenced on HiSeq4000 platform.

RNA-seq data analysis

Before alignment, raw data were first trimmed to remove reads with more than 10% low

quality bases and to trim adaptors. Then the clean reads were mapped to mouse reference genome (mm10) with Tophat (2.0.12) with default settings (Trapnell et al., 2009). HTSeq (0.6.1) was used to do the reads counting, and then RefSeq gene expression level was estimated by RPKM method (Reads per kilobase transcriptome per million reads). Data of RNA-seq of S/L-ESCs and EpiSCs (GSE119985) were downloaded from previous study. Differentially expressed genes (DEGs) in different samples were determined by edgeR package with fold-change $\geqslant$ 2 and p value $\leqslant$ 0.5 (Robinson et al., 2010). Unsupervised hierarchical clustering (UHC) analysis was performed by the R hclust function. Heatmaps of select genes were performed using R heatmap.2 function. Principal component analysis (PCA) analysis was performed with the R prcomp function. Gene ontology analysis was performed using Metascape (http://metascape.org). Trend analysis of DEGs was performed using Short Time-series Expression Miner (STEM) software (Ernst and Bar-Joseph, 2006).

Genomic DNA isolation and WGBS library preparation

Following the manufacturer's instructions, genomic DNA was extracted from stem cells using the DNeasy Blood & Tissue Kit (Qiagen). Remaining RNA was removed by treating with RNase A. Three replicated samples from each of these stem cells were used for library preparation to ensure repeatability of experiment. In short, 2 μg of genomic DNA spiked with 10 ng of lambda DNA were fragmented to about 300 bp with Covaris S220. Next, end repair and A-ligation were performed to the DNA fragments. Methylated Adaptor (NEB) was then ligated to the DNA fragments. In order to reach >99% bisulfite conversion, the adaptor-ligated DNA was treated twice using EZ-96 DNA Methylation-Direct™ MagPrep (Zymo Research). The resulting single-strand DNA fragments were amplified by 4 PCR cycles using the KAPA HiFi HotStart Uracil+ ReadyMix (2×). At last, the libraries were sequenced on HiSeq4000 platform to generate 150-bp paired-end reads.

DNA methylation analysis

Whole genome bisulfite sequencing reads were trimmed with Trim Galore (v0.3.3) to remove adaptors and low quality bases. Then we used Bismark (v0.7.6) (Krueger and Andrews, 2011) to map the clean reads to mouse reference genome (mm10) with a paired-end and

non-directional model, then the unmapped reads were realigned to the same genome with a single-end and non-directional model. PCR duplications were removed with command 'samtools rmdup' (v0.1.18). WGBS data of 2i/L-ESCs and S/L-ESCs were downloaded from previous study (GSE98517) (Hackett et al., 2017) and identically processed. The global DNA methylation level, estimated using a 2 kb window across the genome, and DNA methylation level in each genomic regions was estimated based on 3x CpG sites (CpGs covered more than 3 times). Only regions with more than 3 CpGs covered were retained. Genomic annotation, like exons, introns and repeat regions were downloaded from UCSC genome browser. Promoters were regions 1 kb upstream and 0.5 kb downstream of transcription start sites (TSS). Imprint control regions (ICR) were obtained from previous study (Xie et al., 2012), for the low coverage of published S/L-ESCs data, DNA methylation level on ICRs were estimated based on 1x CpG sites. Locations of ICRs were converted with UCSC LiftOver from mm9 to mm10.

Statistical analysis

All values are depicted as mean ± SD. Statistical parameters including statistical analysis, statistical significance, and n value are reported in the Figure legends and Expanded View Figure legends. Statistical analyses were performed using Prism Software (GraphPad Prism version 6). The significance of differences was measured by an unpaired two-tailed Student's *t* test was employed. A value of $p < 0.05$ was considered significant.

Accession numbers

These RNA-seq data are available through the NCBI Sequence Read Archive (SRA) under the ID PRJNA601004 (https://dataview.ncbi.nlm.nih.gov/object/PRJNA601004?reviewer=ckal7bagkptogce20v1qf6mp2o). WGBS data have been deposited in the NCBI Gene expression omnibus (GEO) under accession number GSE142799 (https://www.ncbi.nlm.nih.gov/geo/query/acc.cgi?acc=GSE142799). All data that support the conclusions in the study are available from the authors on reasonable request.

Figure 1

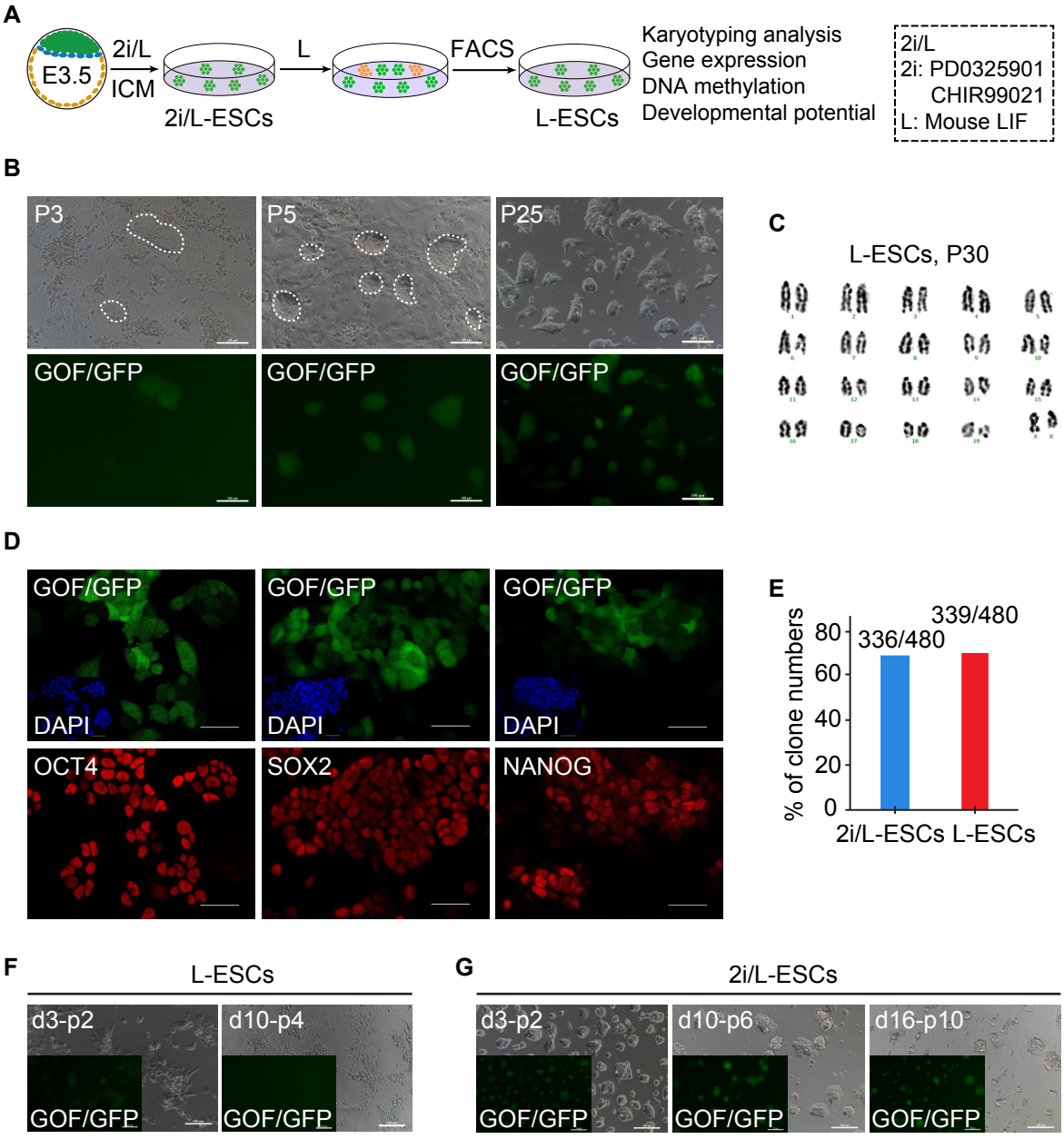
A
E3.5
2i/L
ICM
2i/L-ESCs
L
FACS
L-ESCs
Karyotyping analysis
Gene expression
DNA methylation
Developmental potential
2i/L
2i: PD0325901
CHIR99021
L: Mouse LIF
B
P3
P5
P25
GOF/GFP
C
L-ESCs, P30
D
DAPI
OCT4
SOX2
NANOG
E
% of clone numbers
336/480
339/480
2i/L-ESCs
L-ESCs
F
L-ESCs
d3-p2
d10-p4
G
2i/L-ESCs
d3-p2
d10-p6
d16-p10

Figure 2

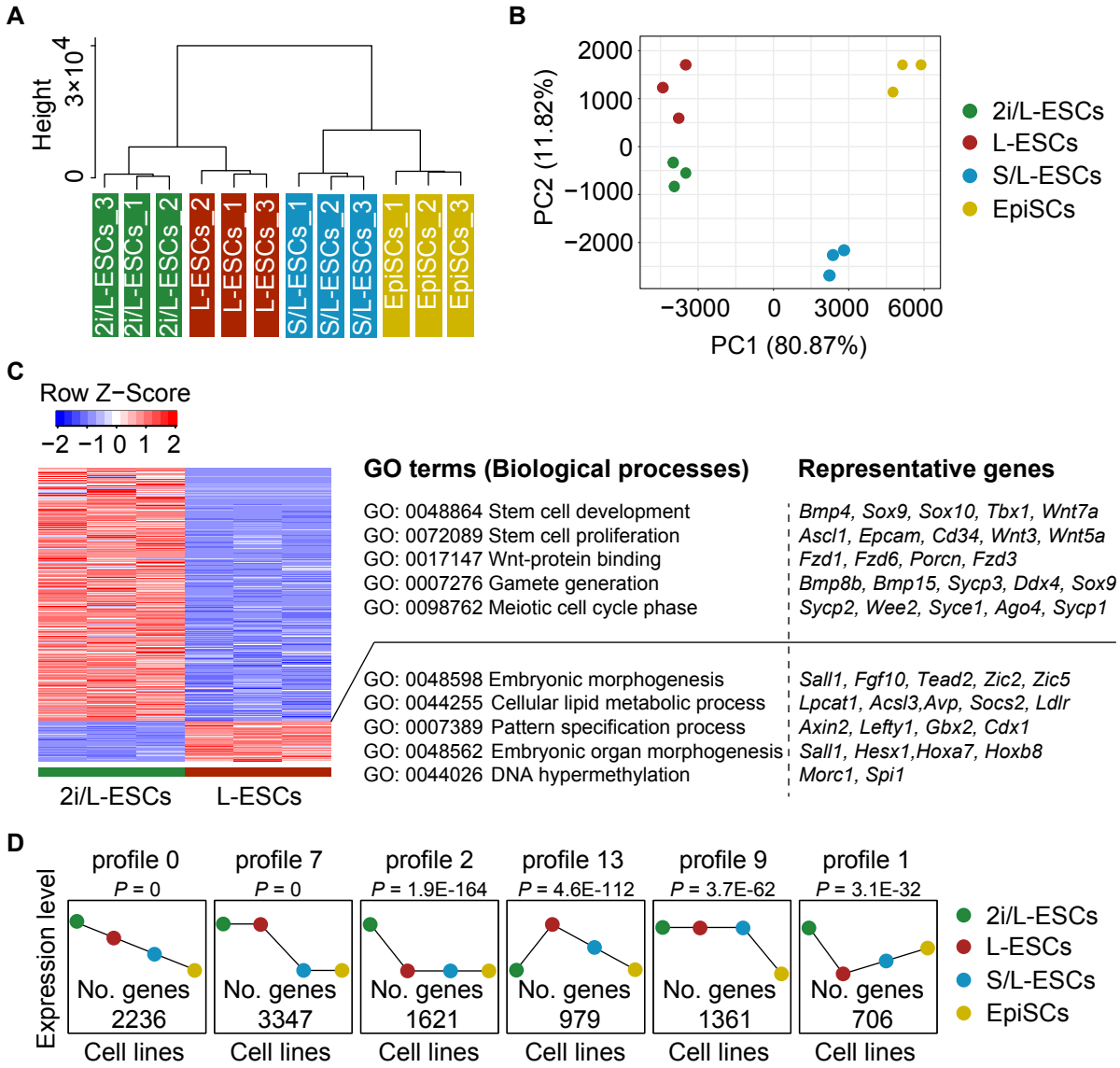
A
Height
3×10^4
0
2i/L-ESCs_3
2i/L-ESCs_1
2i/L-ESCs_2
L-ESCs_2
L-ESCs_1
L-ESCs_3
S/L-ESCs_1
S/L-ESCs_2
S/L-ESCs_3
EpiSCs_1
EpiSCs_2
EpiSCs_3
B
PC2 (11.82%)
2000
1000
0
−1000
−2000
−3000
0
3000
6000
PC1 (80.87%)
2i/L-ESCs
L-ESCs
S/L-ESCs
EpiSCs
C
Row Z−Score
−2 −1 0 1 2
2i/L-ESCs
L-ESCs
GO terms (Biological processes)
Representative genes
GO: 0048864 Stem cell development
Bmp4, Sox9, Sox10, Tbx1, Wnt7a
GO: 0072089 Stem cell proliferation
Ascl1, Epcam, Cd34, Wnt3, Wnt5a
GO: 0017147 Wnt-protein binding
Fzd1, Fzd6, Porcn, Fzd3
GO: 0007276 Gamete generation
Bmp8b, Bmp15, Sycp3, Ddx4, Sox9
GO: 0098762 Meiotic cell cycle phase
Sycp2, Wee2, Syce1, Ago4, Sycp1
GO: 0048598 Embryonic morphogenesis
Sall1, Fgf10, Tead2, Zic2, Zic5
GO: 0044255 Cellular lipid metabolic process
Lpcat1, Acsl3,Avp, Socs2, Ldlr
GO: 0007389 Pattern specification process
Axin2, Lefty1, Gbx2, Cdx1
GO: 0048562 Embryonic organ morphogenesis
Sall1, Hesx1,Hoxa7, Hoxb8
GO: 0044026 DNA hypermethylation
Morc1, Spi1
D
Expression level
profile 0
P = 0
No. genes
2236
profile 7
P = 0
No. genes
3347
profile 2
P = 1.9E-164
No. genes
1621
profile 13
P = 4.6E-112
No. genes
979
profile 9
P = 3.7E-62
No. genes
1361
profile 1
P = 3.1E-32
No. genes
706
Cell lines
2i/L-ESCs
L-ESCs
S/L-ESCs
EpiSCs

Figure 3

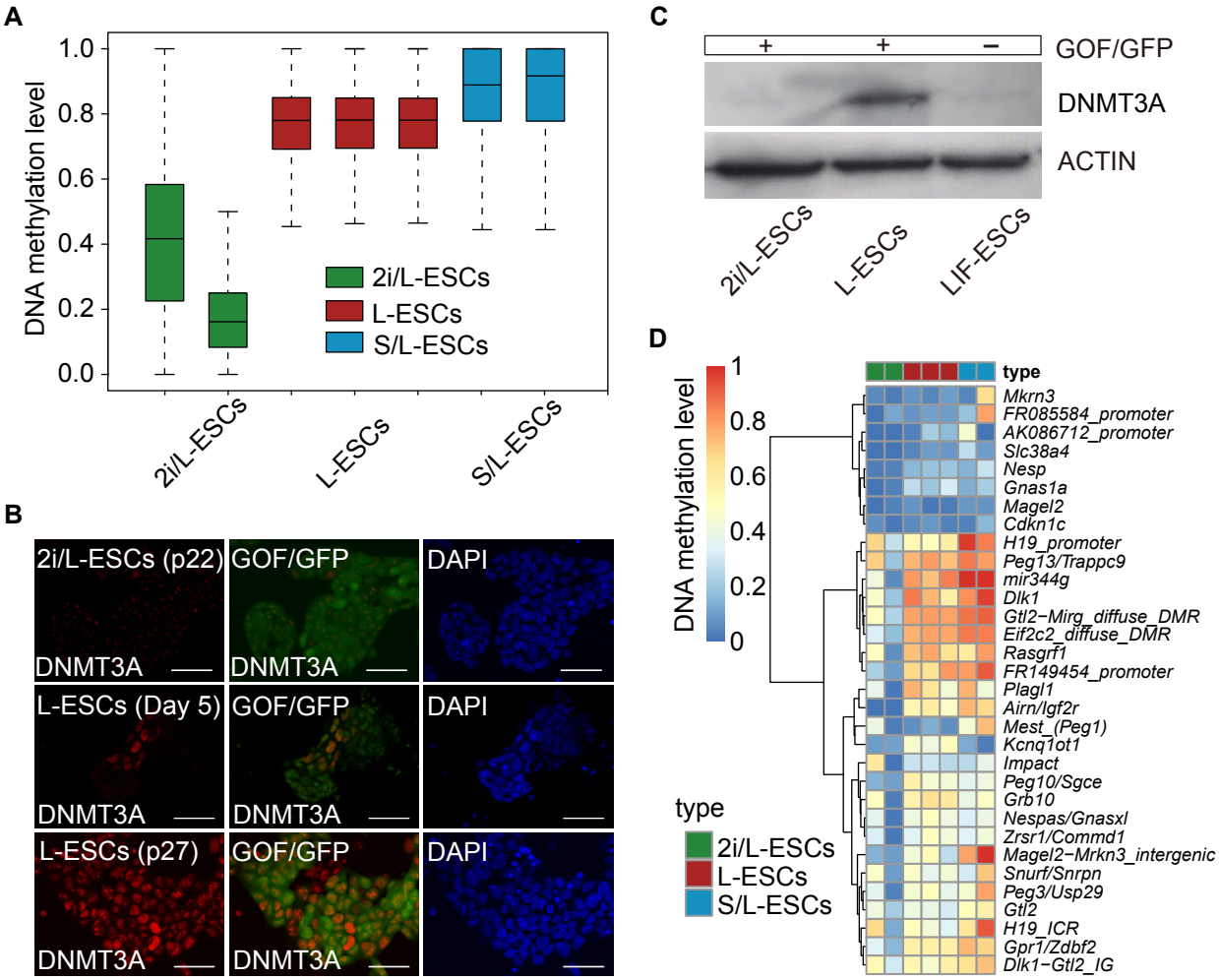
A
DNA methylation level
1.0
0.8
0.6
0.4
0.2
0.0
2i/L-ESCs
L-ESCs
S/L-ESCs
2i/L-ESCs
L-ESCs
S/L-ESCs
B
2i/L-ESCs (p22)
GOF/GFP
DAPI
DNMT3A
L-ESCs (Day 5)
L-ESCs (p27)
C
GOF/GFP
DNMT3A
ACTIN
2i/L-ESCs
L-ESCs
LIF-ESCs
D
DNA methylation level
type
Mkrn3
FR085584_promoter
AK086712_promoter
Slc38a4
Nesp
Gnas1a
Magel2
Cdkn1c
H19_promoter
Peg13/Trappc9
mir344g
Dlk1
Gtl2−Mirg_diffuse_DMR
Eif2c2_diffuse_DMR
Rasgrf1
FR149454_promoter
Plagl1
Airn/Igf2r
Mest_(Peg1)
Kcnq1ot1
Impact
Peg10/Sgce
Grb10
Nespas/Gnasxl
Zrsr1/Commd1
Magel2−Mrkn3_intergenic
Snurf/Snrpn
Peg3/Usp29
Gtl2
H19_ICR
Gpr1/Zdbf2
Dlk1−Gtl2_IG
2i/L-ESCs
L-ESCs
S/L-ESCs

Figure 4

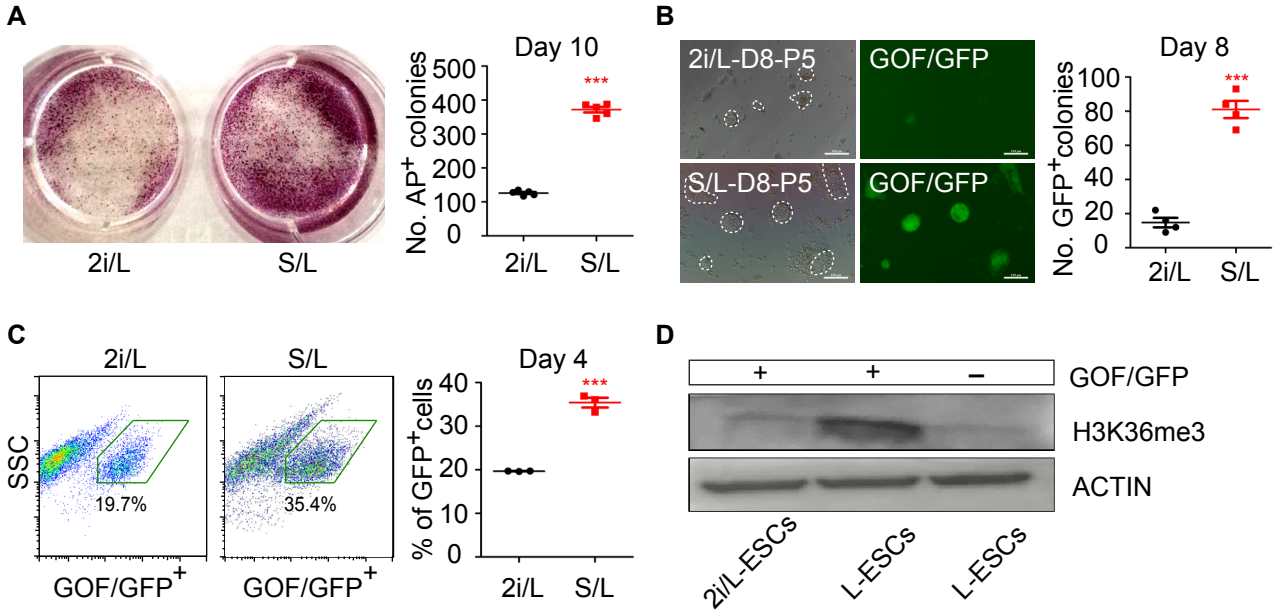
A
2i/L
S/L
Day 10
No. AP+ colonies
500
400
300
200
100
0
***
2i/L
S/L
B
2i/L-D8-P5
GOF/GFP
S/L-D8-P5
GOF/GFP
Day 8
No. GFP+ colonies
100
80
60
40
20
0
***
2i/L
S/L
C
2i/L
S/L
SSC
19.7%
35.4%
GOF/GFP+
GOF/GFP+
Day 4
% of GFP+ cells
40
30
20
10
0
***
2i/L
S/L
D
+
+
–
GOF/GFP
H3K36me3
ACTIN
2i/L-ESCs
L-ESCs
L-ESCs

Figure 5

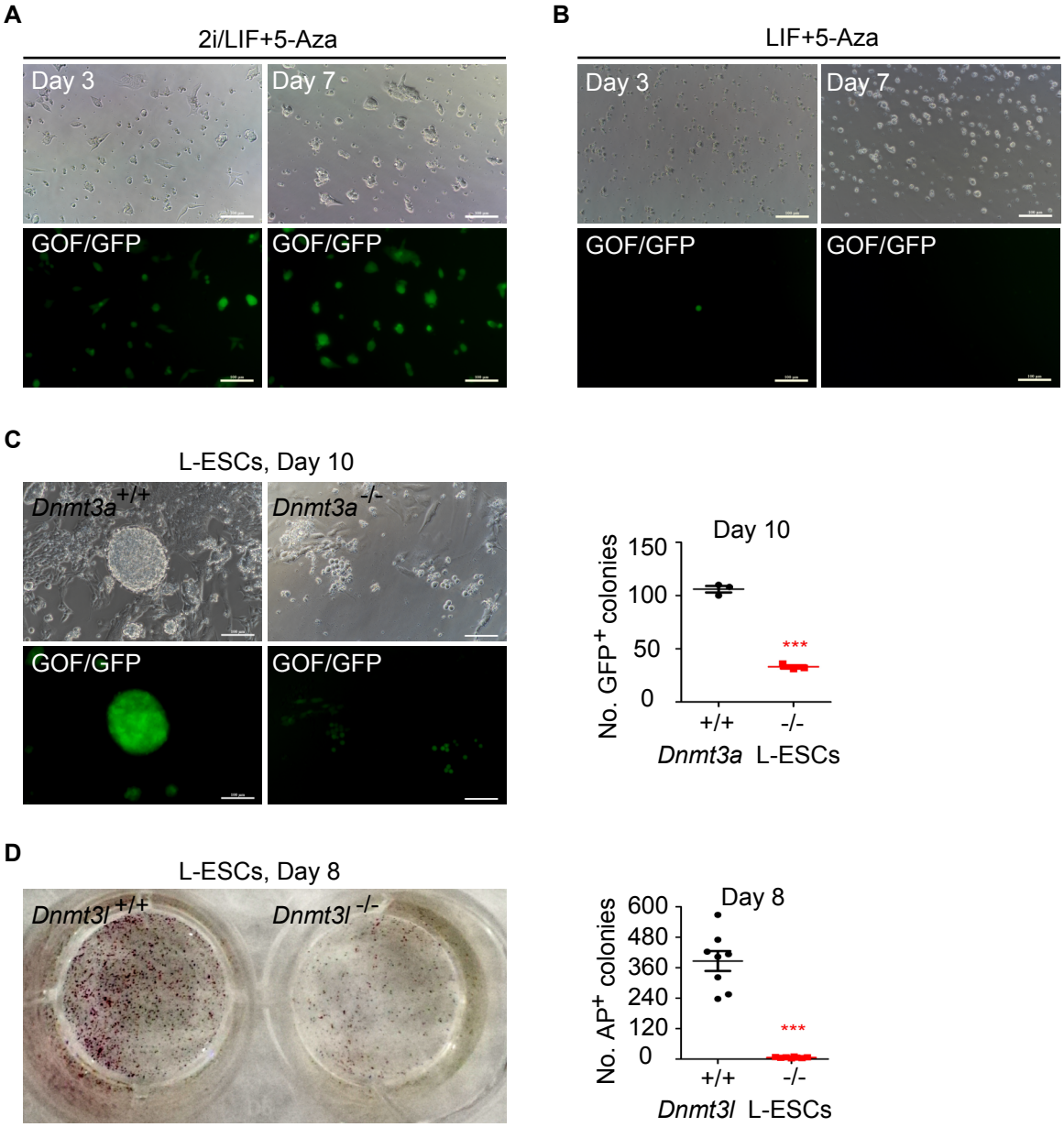
A
2i/LIF+5-Aza
Day 3
Day 7
GOF/GFP
GOF/GFP
B
LIF+5-Aza
Day 3
Day 7
GOF/GFP
GOF/GFP
C
L-ESCs, Day 10
Dnmt3a +/+
Dnmt3a -/-
GOF/GFP
GOF/GFP
Day 10
No. GFP+ colonies
150
100
50
0
***
+/+
-/-
Dnmt3a L-ESCs
D
L-ESCs, Day 8
Dnmt3l +/+
Dnmt3l -/-
Day 8
No. AP+ colonies
600
480
360
240
120
0
***
+/+
-/-
Dnmt3l L-ESCs

Figure 6

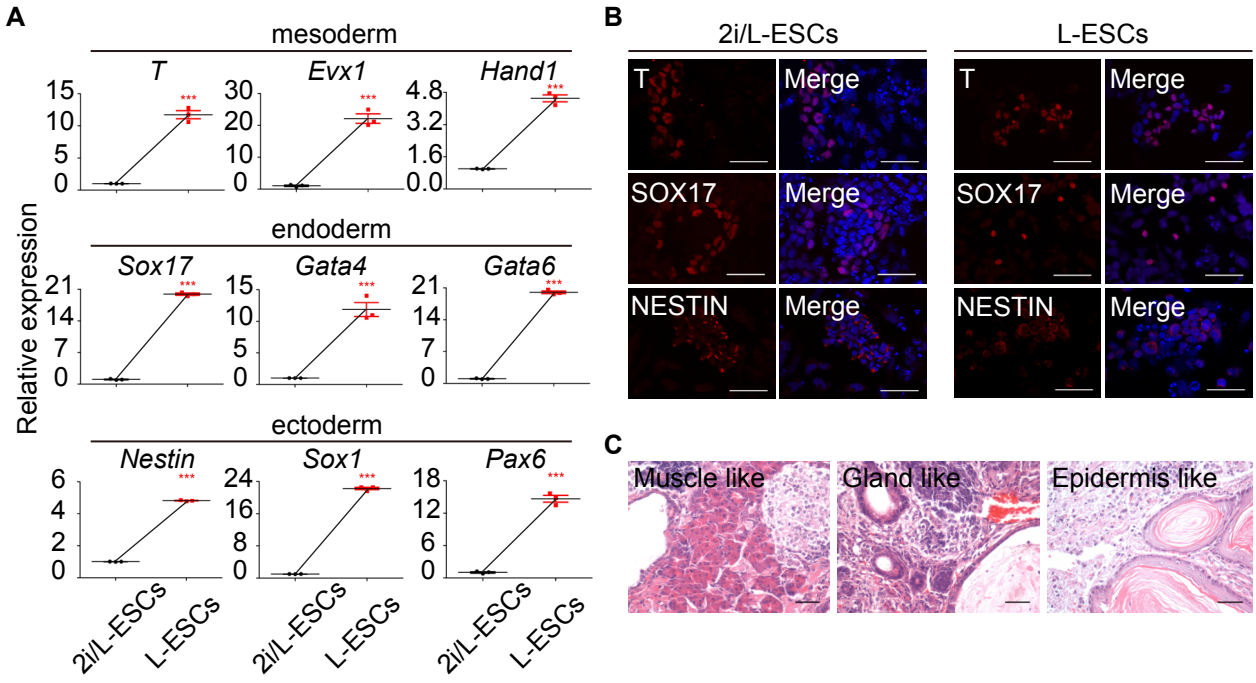
A
mesoderm
T
Evx1
Hand1
endoderm
Sox17
Gata4
Gata6
ectoderm
Nestin
Sox1
Pax6
Relative expression
2i/L-ESCs
L-ESCs
B
2i/L-ESCs
L-ESCs
T
Merge
SOX17
NESTIN
C
Muscle like
Gland like
Epidermis like

Figure 7

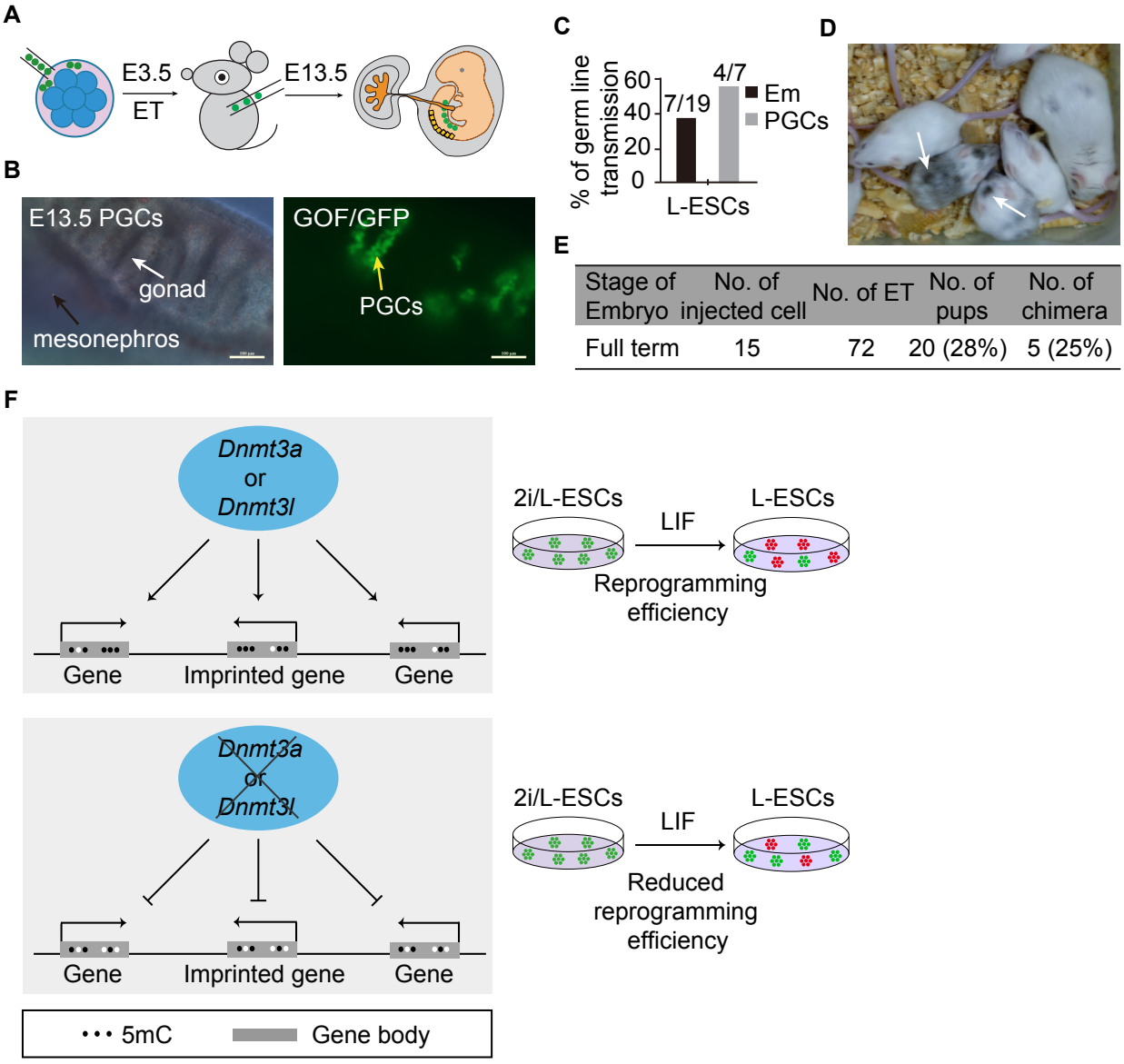

Stage of Embryo	No. of injected cell	No. of ET	No. of pups	No. of chimera
Full term	15	72	20 (28%)	5 (25%)

Figure S1

A

Cell line	Original medium	Derived L-ESCs	Repeated times
W1	2i/LIF	yes	1
W2	2i/LIF	yes	3
W4	2i/LIF	yes	2
W5	2i/LIF	yes	2
W6	2i/LIF	yes	3
SQ3.3	2i/LIF	yes	3
Total	2i/LIF	yes	16

B

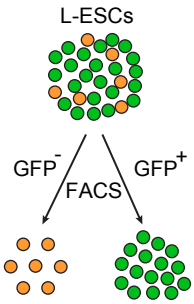

Cell line	medium	No. Sorting	Passage	GFP+ (%)
W2	LIF	1	P23	66
		2	P29	98
		3	P31	99
W6	LIF	1	P14	56
		2	P18	78
		3	P21	91
		4	P33	78
		5	P42	98
W4	LIF	1	P34	97
W5	LIF	1	P34	98
W2	2i/LIF	1	P15	98

C

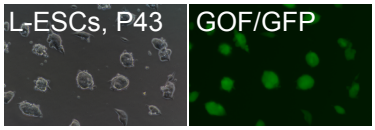

D

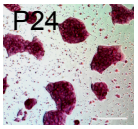

E

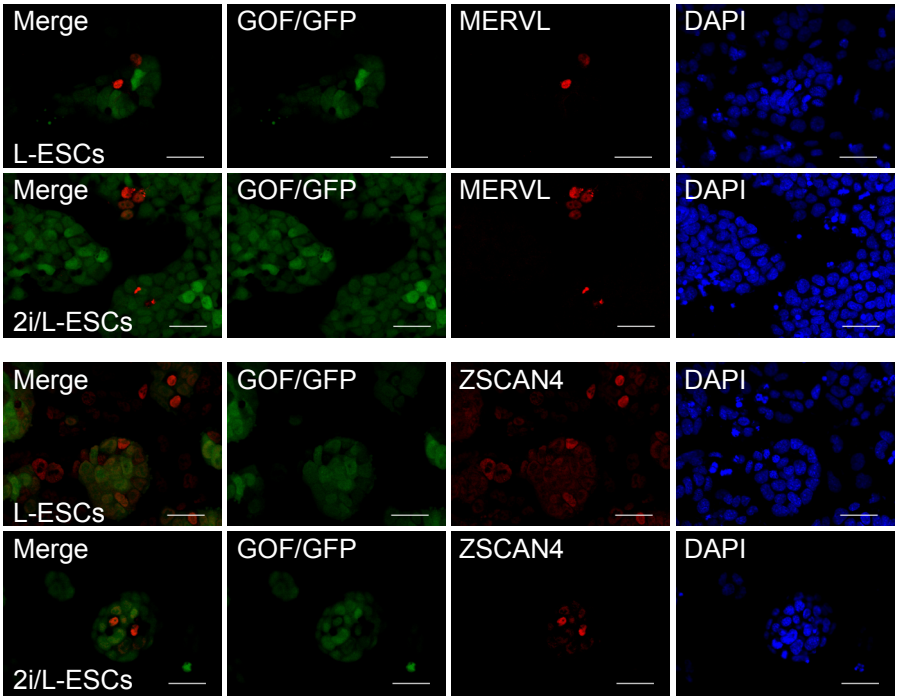

F

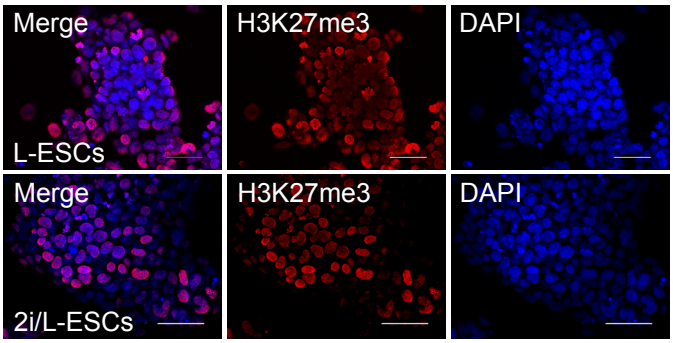

Figure S2

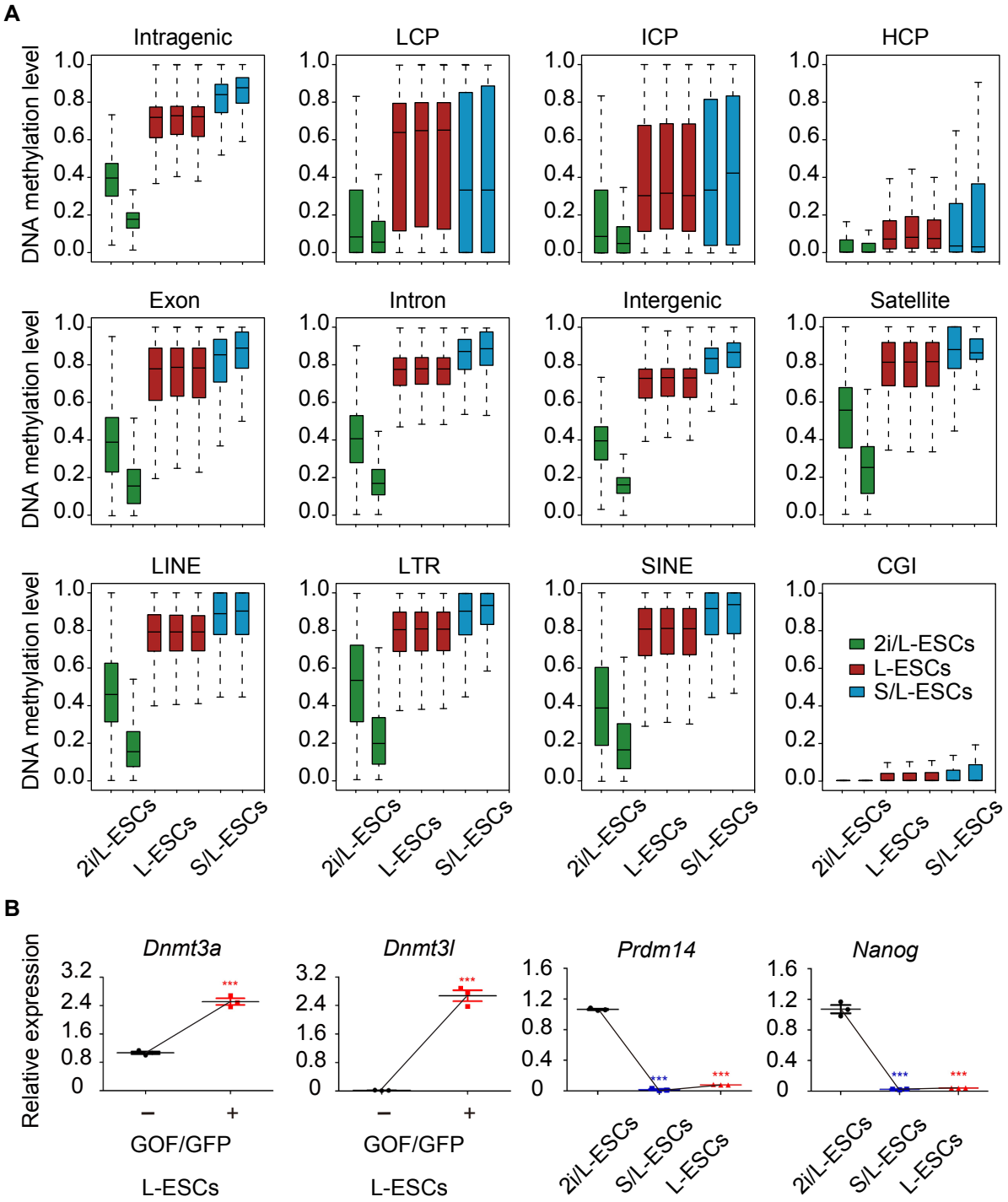
A
Intragenic
LCP
ICP
HCP
Exon
Intron
Intergenic
Satellite
LINE
LTR
SINE
CGI
DNA methylation level
1.0
0.8
0.6
0.4
0.2
0.0
2i/L-ESCs
L-ESCs
S/L-ESCs
B
Relative expression
Dnmt3a
Dnmt3l
Prdm14
Nanog
3.2
2.4
1.6
0.8
0
1.2
0.4
***
−
+
GOF/GFP
L-ESCs

Figure S3

A

Cell line	Original medium	S/L induction and L-ESCs reprogramming	Repeated times
W2	2i/L	yes	3
W6	2i/L	yes	4
W4	2i/L	yes	4
SQ3.3	2i/L	yes	2
J1	S/L	yes	3
Dnmt3l-/-	S/L	yes	3

B

Cell line	W5		329			
Culture medium	2i+LIF	2i+LIF	ABCL	ABCL	LIF	LIF
Number of AP^+ colonies	1673	1862	3425	3672	1660	1548

C

Cell line	Original medium	Reprogrammed L-ESCs	Repeated times
G3	ABCL	yes	3
G3-AH	ABCL	yes	2
G12	ABCL	yes	1
329	ABCL	yes	3
Dnmt3a-/-	ABCL	yes	2

Figure S4

A

2i/LIF+5-Aza

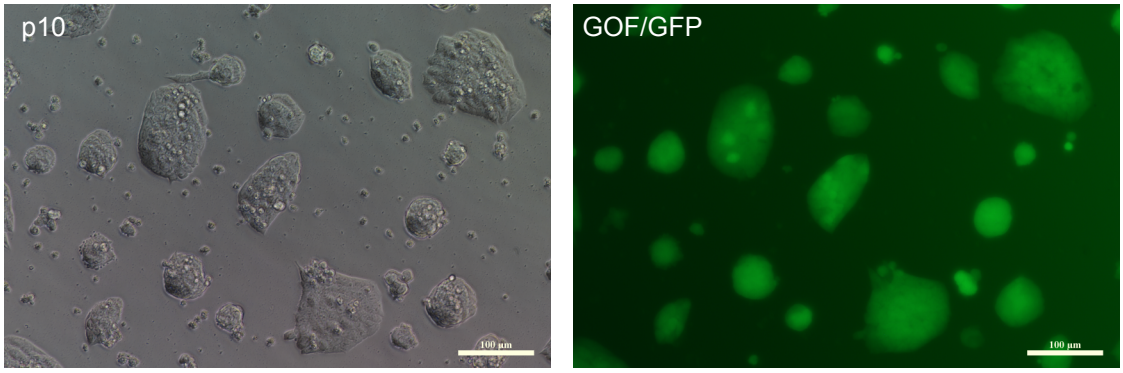

B

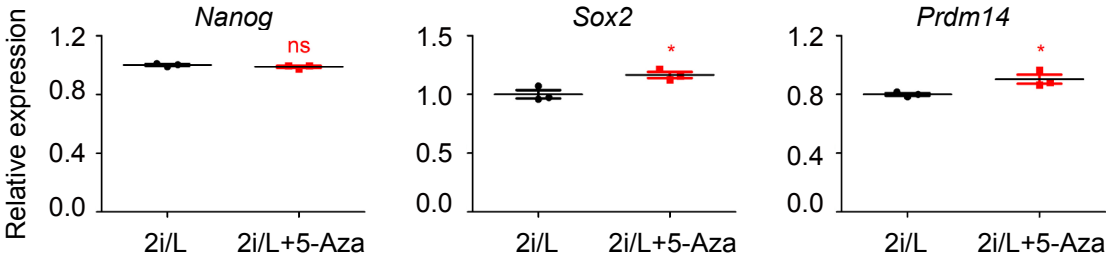

Figure S5

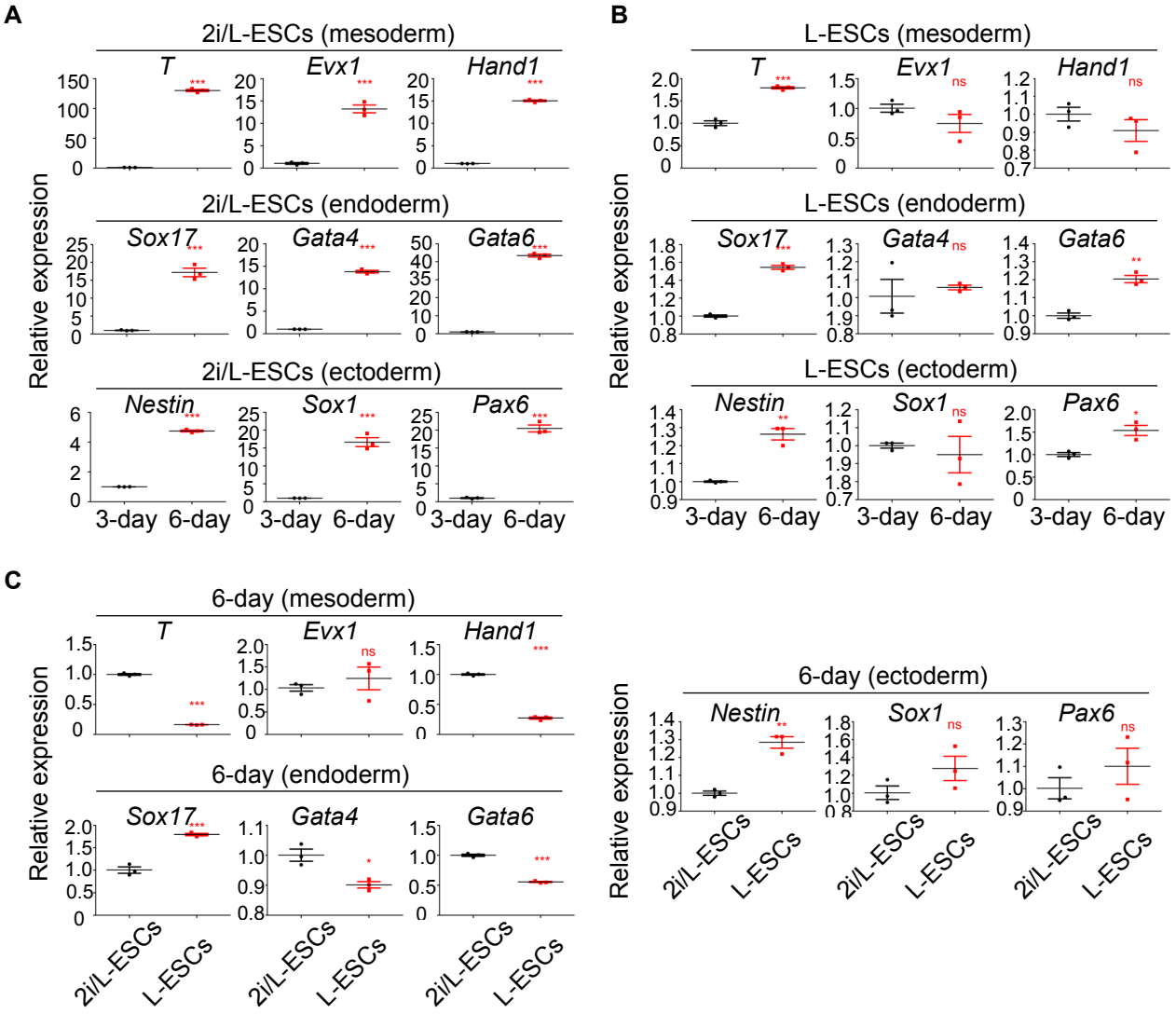
A
2i/L-ESCs (mesoderm)
T
Evx1
Hand1
2i/L-ESCs (endoderm)
Sox17
Gata4
Gata6
2i/L-ESCs (ectoderm)
Nestin
Sox1
Pax6
Relative expression
3-day
6-day
B
L-ESCs (mesoderm)
L-ESCs (endoderm)
L-ESCs (ectoderm)
C
6-day (mesoderm)
6-day (endoderm)
6-day (ectoderm)
2i/L-ESCs
L-ESCs

Table S1. Related to Figure 3A, WGBS data coverage and conversion efficiency

Sample	Total sequenced bases(Gb)	Total sequenced reads	Reads after trimming	Unique mapped reads	Mapping efficiency	Coveraged bases (1x)
L-ESCs_rep1	23.36	155,760,956	151,382,966	98,603,675	65.14%	2,317,989,827
L-ESCs_rep2	26.20	174,654,234	168,555,054	106,718,870	63.31%	2,334,743,972
L-ESCs_rep3	24.60	163,969,284	158,835,308	103,120,363	64.92%	2,346,240,160

Sample	Fraction of genome covered	Bisulfite Conversion Rate	No.of unique CpG covered (1x)	No.of unique CpG covered (3x)	No.of unique CpG covered (5x)
L-ESCs_rep1	85.05%	99.96%	30,757,370	14,829,901	5,277,450
L-ESCs_rep2	85.66%	99.96%	30,976,871	15,454,751	5,806,380
L-ESCs_rep3	86.08%	99.96%	31,620,932	15,560,785	5,654,681

Table S2. Related to materials and methods

RT-qPCR primers

Gene name	Forward Primer	Reverse Primer
Nanog	CTTTCACCTATTAAGGTGCTTGC	TGGCATCGGTTCATCATGGTAC
Prdm14	CCTGAACAAGCACATGAGA	TGCACTTGAAGGGCTTCTCT
Gata4	TTCCTCTCCCAGGAACATCAAA	GCTGCACAACTGGGCTCTACTT
Gata6	TGCTGGAAATTGCAACAAACC	GTCACGTGGTACAGGCGTCA
Sox17	GTCAACGCCTTCCAAGACTTG	GTAAAGGTGAAAGGCGAGGTG
Brachyury	GAACCTCGGATTCACATCGT	TTCTTTGGCATCAAGGAAGG
Evx1	CCAGTGACCAGATGCGCCGATAC	TCCTTCATGCGCCGGTTCT
Hand1	TCAAAAAGACGGATGGTGGT	GCGCCCTTTAATCCTCTTCT
Dnmt3a	GACTCGCGTGCAATAACCTTAG	GGTCACTTTCCCTCACTCTGG
Dnmt3l	CGGAGCATTGAAGACATC	CATCATCATACAGGAAGAGG
Sox2	GCGGCGGAAAACCAAGA	CCGGGAAGCGTGTACTTATCC
Nestin	CTCGAGCAGGAAGTGGTAGG	TTGGGACCAGGGACTGTTAG
Sox1	GGCCGAGTGGAAGGTCATGT	TCCGGGTGTTCCTTCATGTG
Pax6	GCAGATGCAAAAGTCCAGGTG	CAGGTTGCGAAGAACTCTGTTT
GAPDH	ATGGTGAAGGTCGGTGTGAAC	TCGCTCCTGGAAGATGGTGATG

Guide RNA sequences

Dnmt3a sgRNA1	CACCGCTCATACTCAGGCTCATCGT
Dnmt3a sgRNA1-CS	AAACACGATGAGCCTGAGTATGAGC
Dnmt3a sgRNA2	CACCGGACCCTGCTTCTCCGACTG
Dnmt3a sgRNA2-CS	AAACCAGTCGGAGAAGCAGGGTCC

Genotyping primer

Dnmt3a 89925 Forward Primer	GCCTTGGCTGTGTGAGATTTG
Dnmt3a 90586 Reverse Primer	ATCCTGGAGCCCCAAAGAGC